An analysis of the variability of δ^{13}C in macroalgae from the Gulf of California: indicative of carbon concentration mechanisms and isotope discrimination during carbon assimilation

Roberto Velázquez-Ochoa[a], María Julia Ochoa-Izaguirre[b], Martín F. Soto-Jiménez[c*]

[a]Posgrado en Ciencias del Mar y Limnología, Universidad Nacional Autónoma de México, Unidad Académica Mazatlán, Mazatlán, Sinaloa 82040, México

[b]Facultad de Ciencias del Mar, Universidad Autónoma de Sinaloa. Paseo Claussen s/n, Mazatlán, Sinaloa 82000, México

[c]Unidad Académica Mazatlán, Instituto de Ciencias del Mar y Limnología, Universidad Nacional Autónoma de México (UAM-ICMyL-UNAM), Mazatlán Sinaloa, 82040, México.

Correspondent author:

Telephone number: +52 (669) 9852845 to 48.

Fax number: +52 (669) 9826133

E-mail: martin@ola.icmyl.unam.mx

Abstract

The isotopic composition of carbon in macroalgae ($\delta^{13}C$) is highly variable, and its prediction complex concerning terrestrial plants. The determinants of $\delta^{13}C$-macroalgal variations were analyzed in a large stock of specimens that vary in taxa and morphology, collected in shallow marine habitats in the Gulf of California (GC) with distinctive environmental conditions. A large $\delta^{13}C$ variability (-34.6‰ to -2.2‰) was observed. Life forms (taxonomy 57%, morphology and structural organization 34%) explains the variability related to the carbon use physiology. Environmental conditions influenced the $\delta^{13}C$-macroalgal values, but did not change the physiology, which is most likely inherently species-specific. Measurements of $\delta^{13}C$ were used as indicative of the presence or absence of carbon concentrating mechanisms (CCMs) and as integrative values of the isotope discrimination during carbon assimilation in the lifecycle macroalgae. Based on $\delta^{13}C$ signals, macroalgae were classified in four strategies relatives to the capacity of CCM: 1) HCO_3^- uptake ($\delta^{13}C$>-10‰), 2) using a mix of CO_2 and HCO_3^- uptake (-10<$\delta^{13}C$>-30‰), 3) CO_2 diffusive entry ($\delta^{13}C$<-30‰), and 4) calcifying species ($\delta^{13}C$>-10‰). Most species showed a $\delta^{13}C$ that indicates a CCM using a mix of CO_2 and HCO_3^- uptake. HCO_3^- uptake is also widespread among GC macroalgae, with many Ochrophyta species. Few species belonging to Rhodophyta relied on CO_2 diffusive entry exclusively, while calcifying macroalgae species using HCO_3^- included only *Amphiroa* and *Jania*. The isotopic signature evidenced the activity of CCM, but it was inconclusive about the preferential uptake of HCO_3^- and/or CO_2 in photosynthesis and the CCM type expressed in macroalgae. In the carbon use strategies study, diverse and species-specific, complementary techniques to the isotopic tools are required.

Keywords: $\delta^{13}C$-macroalgal, carbon-concentrating mechanisms, CO_2 diffusive proxy

1. Introduction

Macroalgae show a wide diversity of thallus morphologies (e.g., filamentous, articulated, flattened), structural organization (e.g., surface area/volume ratio), and various photosynthetic pigments (e.g., Chlorophyll *a*, *b*, phycocyanin) (Lobban and Harrison, 1994). According to the predominant pigment contents in the thallus, macroalgae are classified in three Phyla. Considering the interaction of morphologies and photosynthetic pigments, are classified in dozens of groups (Littler and Littler, 1980; Littler & Arnold, 1982; Balata et al., 2011). For example, the mixture of chlorophyll (*a*, *b*) and carotenoids is dominant in Chlorophyta; chlorophyll (*a*, *c*) and fucoxanthin carotenoid is dominant in Ocrophyta, while Rhodophyta contains chlorophyll (*a*, *d*), carotenoid, and a mixture of phycobilin (e.g., phycocyanin, phycoerythrin, allophycocyanin) (Bold and Wynne, 1978; Masojidek et al., 2004; Gateau et al., 2017). Both traits work as an excellent approximation to explain the fundamentals of metabolism, growth, zonation, and colonization (Littler and Littler, 1980; Littler and Arnold, 1982; Nielsen and Sand-Jensen, 1990; Vásquez-Elizondo and Enríquez, 2017).

In marine environments, where pH~8.1±1, HCO_3^- accounts for 98% of the total dissolved inorganic carbon (DIC) due to the low diffusion rate of CO_2 in seawater, resulting in a high HCO_3^-:CO_2 ratio (150:1) (Sand-Jensen and Gordon, 1984). The limitations to growth imposed by low CO_2 concentrations in seawater are compensated by carbon concentrating mechanisms (CCMs) in most macroalgae that increase the internal inorganic carbon concentration near the site of RuBisCo activity (Giordano et al., 2005). Therefore, the absorption of HCO_3^- by most macroalgae is the primary source of inorganic carbon for photosynthesis, but some species depend exclusively on the use of dissolved CO_2 that enters cells by diffusion (Maberly et al., 1992; Beardall and Giordano, 2002; Raven et al., 2002a, b; Giordano et al., 2005). Hence, macroalgal species with productivity limited by lacking CCM's (have low plasticity for carbon inorganic forms uptake) seems to be restricted to subtidal habitats and composed mainly by red macroalgae (but without a morphological patron apparent) (Cornwall et al., 2015, Kübler and Dungeon, 2015). The rest of the macroalgae with CCM occupies from the intertidal to the deep subtidal.

The habitat features and environmental conditions in marine ecosystems modify the main macroalgae photosynthesis drivers, such as light (Anthony et al., 2004; Johansson and Snoeijs, 2014), DIC (Zeebe and Wolf-Gladrow, 2001; Brodeur et al., 2019), and inorganic nutrients (Teichberg et al., 2010; Ochoa-Izaguirre and Soto-Jiménez, 2015). These factors could generate negative consequences for their productivity, principally when they cause resources limitation. Each factor varies from habitat to habitat (e.g., local scale: from intertidal to subtidal and global scale: from temperate to tropical regions), and as in response to these environmental changes, macroalgae can modulate their photosynthetic mechanism (Lapointe and Duke, 1984; Dudgeon et al., 1990; Kübler and Davison 1993, Young and Beardall., 2005). The modulation, to increase their photosynthetic activity (up-and-down-regulation processes), implies a physiological acclimation enhancing the transport of DIC (CO_2, HCO_3^-) into the cell and its fixation rates (Madsen and Maberly, 2003; Klenell et al., 2004; Zou et al., 2004; Giordano et al., 2005; Enríquez and Rodriguez-Román, 2006; Rautenberger et al., 2015).

The $\delta^{13}C$ on the thallus of marine macrophytes are indicative of the carbon source used (CO_2 or HCO_3^-) in photosynthesis and allow infer the presence or absence of CCM's (Maberly et al., 1992; Raven et al., 2002a; Giordano et al., 2005). However, the isotopic signature may be inconclusive for determine the preference of the carbon source (Roleda and Hurd, 2012). Also, the $\delta^{13}C$ signal in the algal thallus can be used as an indicator of the physiological state of photosynthetic metabolism (Kim et al., 2014; Kübler and Dungeon, 2015). For example, $\delta^{13}C$ variability depends, in part, on the life forms as taxonomy, morphology, and structural organization (Mercado et al., 2009, Marconi et al., 2011, Roleda and Hurd, 2012; Lovelock et al., 2020). $\delta^{13}C$ is also modulated by the interaction to environmental conditions (e.g., light, DIC, and nutrients) (Cornelisen et al., 2007; Dudley et al., 2010; Carvalho et al., 2010ab; Roleda and Hurd, 2012; Mackey et al., 2015; Rautenberger et al., 2015). In this study, our objective was to investigate the contributions of life forms, the changes in the habitat features, and environmental conditions to the $\delta^{13}C$ macroalgal variability in communities in the Gulf of California (GC). To reach our objective, we collected a large stock of macroalgae specimens of a diversity of species characterized by various morphological and physiological properties. Besides high diversity, in terms of life forms, we selected various shallow marine habitats along a latitudinal gradient in the GC or the sample collection, characterized by unique and changing environmental factors. The GC features abundant and diverse macroalgae populations, acclimated and adapted to diverse habitats with environmental conditions, determining the light, DIC, and nutrients availability. The $\delta^{13}C$ signal from the thallus of macroalgae were used as indicative of the presence or absence of CCMs and as integrative values of the isotope discrimination during carbon assimilation and respiration along lifecycle macroalgae in macroalgae communities in the GC in the function of taxa and environmental factors (Maberly et al., 1992; Raven et al., 2002a; Hepburn et al., 2011; Díaz-Pulido et al., 2016). Because the GC is a subtropical zone with high irradiance and specimens were collected in the intertidal and shallow subtidal zone, we expect to find a high proportion of species with active uptake HCO_3^- ($\delta^{13}C$>-10‰). A third objective was to explore any geographical pattern in the $\delta^{13}C$ macroalgal along and between the GC bioregions. Previous studies have indicated changes in the $\delta^{13}C$ signal with latitude, mainly related to the light and temperature (Mercado et al., 2009; Marconi et al., 2011; Stepien, 2015; Hofmann and Heesch, 2018; Lovelock et al., 2020). Macroalgae as biomonitors constitute an efficient tool in monitoring programs in large geographical regions (Balata et al., 2011) and for environmental impact assessments (Ochoa-Izaguirre and Soto-Jiménez, 2015).

2. Materials and Methods

2.1. Gulf of California description

The Gulf of California is a subtropical, semi-enclosed sea of the Pacific coast of Mexico, with exceptionally high productivity being the most important fishing region for Mexico and one of the most biologically diverse worldwide marine areas (Zeitzschel, 1969; Espinosa-Carreón and Valdez-Holguín 2007; Lluch-Cota et al., 2007; Páez-Osuna et al., 2017). GC represents only 0.008% of the area covered by the seas of the planet (265,894 km^2, 150 km wide, and 1000 km long covering >9 degrees latitude) but has a high physiographic diversity and is biologically mega-diverse with many endemic species, including ~ 766 macrofauna species and/or sub-species where the major number belong to Arthropoda (118 spp) and Mollusca (460) taxas (Brusca et al., 2005; Wilkinson et al., 2009; Espinosa-Carreón and Escobedo-Urías, 2017) and 116 macroalgae species (Norris, 1975, 1985; Espinoza-Avalos, 1993).

Regionalization criteria of the GC include phytoplankton distribution (Gilbert and Allen, 1943), topography (Rusnak et al., 1964) and depth (Álvarez-Borrego, 1983), oceanographic characteristics (Roden and Emilson, 1979; Álvarez-Borrego, 1983; Marinone and Lavin 2003), biogeography (Santamaría-del-Ángel et al., 1994), and bio-optical characteristics (Bastidas-Salamanca et al., 2014). The topography is variable along with GC, includes submarine canyons, basins, and variable continental platforms. Besides, GC presents complex hydrodynamic processes, including internal waves, fronts, upwelling, vortices, mixing of tides. The gulf's coastline is divided into three shores: extensive rocky shores, long sandy beaches, numerous scattered estuaries, coastal lagoons, and open muddy bays, tidal flats, and coastal wetlands (Lluch-Cota et al., 2007).

The Gulf of California is different in the north and the south, related to a wide range of physicochemical factors. The surface currents seasonally change direction and flow to the southeast with maximum intensity during the winter and to the northwest in summer (Roden, 1958). The northern part is very shallow (<200 m deep averaged), divided into Upper Gulf, northern Gulf, and Grandes Islas. The surrounding desserts largely influence this region (Norris, 2010) shows marked seasonal changes in coastal surface seawater temperatures (Martínez-Díaz de León et al., 2006; Marinone, 2007). Tidal currents induce a significant cyclonic circulation through June to September and anticyclonic from November to April (Carrillo et al., 2002; Bray, 1988; Velasco-Fuentes and Marinone, 1999; Martínez-Díaz-de-León, 2001). The southern part consists of a series of basins whose depths increase southwards (Fig. 1). The intertidal macroalgae in the southern region are subject to desiccation, mostly during summer. The water column's physicochemical characteristics are highly influenced by the contrasting climatic seasons in the GC, the dry season (nominally from November to May), and the rainy season (from June to October). Annual precipitation (1,080 mm y^{-1}) and evaporation (56 mm y^{-1}) rates registered during the past 40 years were 881±365 mm y^{-1} and 53±7 mm y^{-1}, respectively (CNA, 2012).

Previous macroalgae floristic studies of the GC, report around 669 species, including 116 endemic species (Norris, 1975; Espinoza-Avalos, 1993; Pedroche and Senties, 2003). Many endemic species currently have a wide distribution along the Pacific Ocean coast, but with GC origin (Dreckman, 2002; Aguilar-Rosas et al., 2014). Based on oceanographic characteristics (Roden and Groves, 1959) and in the endemic species distribution (Aguilar Rosas and Aguilar Rosas, 1993; Espinoza-Avalos, 1993), the GC can be classified into three phycofloristic zones: 1) the first zone located from the imaginary line connecting San Francisquito Bay, B.C. to Guaymas, Sonora, with 51 endemic species. 2) the second zone with an imaginary line from La Paz Bay (B.C.S.) to Topolobampo (Sinaloa) with 41 endemic species. 3) the third zone is located with an imaginary line from Cabo San Lucas (B.C.S.) to Cabo Corrientes (Jalisco) with ten endemic species. Besides, 14 endemic species are distributed throughout the GC (Espinoza-Ávalos, 1993). The macroalgal communities are subject to the changing environmental conditions in the diverse habitats in the GC that delimits their zonation, which tolerates a series of anatomical and physiological adaptations to water movement, temperature, sun exposure, and light intensities, low pCO2, desiccation (Espinoza-Avalos 1993).

2.1 Macroalgae sampling

In this study, the GC coastline (21º-30°N latitude) was divided into six coastal sectors based on the three phycofloristic zones along peninsular and continental GC coastlines (Fig. 1a). In each coastal sector, selected ecosystems and representative habitats were sampled based on macroalgae communities' presence and habitat characterization. Habitats were classified by substrate type (e.g., sandy-rock, rocky shore), hydrodynamic (slow to faster water flows), protection level (exposed or protected sites), and immersion level (intertidal or subtidal) (Fig. 1b).

Based on the local environmental factors, 4-5 macroalgae specimens of the most representative species were gathered by hand (free diving) during low tide. A total of 809 composite samples were collected from marine habitats along both GC coastlines. The percentages of specimens collected for the substrate type were sandy-rock 28% and rocky shores 72% based on the habitat features. In the hydrodynamic, 30% of the specimens were collected in habitats with slow to moderate and 70% with moderate to fast water movement. Regarding the protection level, 57% were exposed specimens, and 43% were protected. Finally, 56% were intertidal and 44% subtidal macroalgae organisms concerning the emersion level. About half of the protected specimens were collected in isolated rock pools, which was noted.

In 4-5 sites of each habitat, we measured *in situ* the salinity, temperature, and pH by using a calibrated multiparameter sonde (Y.S.I. 6600V) and the habitat characteristics mentioned above noted. Besides, composite water samples were collected for a complementary analysis of nutrients, alkalinity (and their chemical components), and δ^{13}C-DIC (data non-included). Briefly, the representative habitats were classified by pH levels in >9.0 "alkalinized", 7.9-8.2 'typical' and <7.9 "acidified". Based on the temperature in colder <20ºC, typical 20-25ºC, and warmer >25ºC. 72% of the specimens were collected at typical pH values, 22% alkalinized, and 6% in acidified seawater. Regarding the temperature, about 55% of the specimens were collected at typical, 31% at warmer, and 14% at colder seawaters. Regarding salinity, most of the ecosystems showed typical values for seawater (35.4±0.91 ups, from 34.5 to 36.1 ups). In this study, the collection surveys were conducted during spring (March-April) and dry season (nominally from November to May) from 2008 to 2014. Only in few selected ecosystems located at C1, C2, and C3 sectors, one sampling survey was conducted at the end of the rainy season (nominally from June to October in 2014). Thus, these ecosystems were possible to include habitat with a salinity range varying from estuarine (23.5±3.0 ups) to hypersaline (42.7±7.0 ups) values. These habitats were mainly isolated rock pools, and only a few were sites near tidal channels receiving freshwater discharges. About 95% of the specimens were collected at typical seawater salinity (34-36 ups) and only 1.5 and 3.5% in estuarine (<30 ups) and hypersaline (>37 ups) environments, respectively. Detailed information on the selected shallow marine ecosystems, habitat characterization, and environmental conditions is summarized in the inserted table in Fig. 1.

2.2 Macroalgae processing and analysis of the isotopic composition of carbon

The collected material was washed *in situ* with surface seawater to remove the visible epiphytic organisms, sediments, sand, and debris and then thoroughly rinsed with MilliQ water. The composite samples were double-packed in a plastic bag, labeled with the locality's name and collection date, placed in an ice-cooler box to be kept to 4ºC, and immediately transported to the laboratory UAS-Facimar in Mazatlán. In the field, sample aliquots were also preserved in 4% v/v formaldehyde solution for taxonomic identification to the genus or species level (when possible). The following GC macroalgal flora identification manuals were consulted: Dawson, 1944; 1954; 1956; 1961; 1962; 1963; Setchell and Gardner, 1920; 1924; Abbot and Hollenberg, 1976; Ochoa-Izaguirre et al., 2007; Norris, 2010).

In the laboratory, macroalgae samples were immediately frozen at -30ºC until analysis. Then, samples were freeze-dried at -38ºC and 40 mm Hg for 3 days, upon which they were ground to a fine powder and exposed to HCl vapor for 4 h (acid-fuming) to remove carbonates and dried at 60ºC for 6 h (Harris et al. 2001). Aliquots of ~5 mg were encapsulated in tin cups (5x9 mm) and stored in sample trays until analysis. Macroalgae samples were sent to the Stable Isotope Facility (SIF) at the University of California at Davis, CA, USA. Natural ^{13}C relative abundance relative to ^{12}C in samples was determined with mass spectrometry, using a Carlo Erba elemental analyzer attached to a Finnigan Delta S mass spectrometer equipped with a Europa Scientific stable isotope analyzer (ANCA-NT 20-20) and a liquid/solid preparation unit (PDZ, Europa, Crewz, UK). Isotope ratios of the samples were calculated using the equation δ (‰)=$(R_{sample}/R_{standard}-1)]$x1000, where R=^{13}C/^{12}C. The $R_{standard}$ is relative to the international V-PDB (Vienna PeeDee Belemnite) standard. During the isotopic analysis, the SIF lab used different certified reference materials (e.g., IAEA-600, USGS-40, USGS-41, USGS-42, USGS-43, USGS-61, USGS-64, and USGS-65) for the analytical control quality. The analytical uncertainties reported for the SIF lab were 0.2‰ for δ^{13}C (https://stableisotopefacility.ucdavis.edu/13cand15n.html). We also included triplicate aliquots of several specimens of the same species and condition, collected from one patch, or attached to the same substrate, to assess the method error by sampling and processing procedural. The methodological uncertainties were <0.4‰.

2.3. Analysis of δ^{13}C-macroalgal variability

The variability of δ^{13}C values in macroalgae was analyzed in function of the taxonomy (phylum, genus, and species) and morpho-functional groups (e.g., thallus structure, growth form, branching pattern, and taxonomic affinities; Balata et al. 2011; Ochoa-Izaguirre and Soto-Jiménez, 2015). The carbon fixation strategies in the macroalgae communities of the GC were identified by δ^{13}C (Hepburn et al., 2011; Díaz-Pulido et al., 2016), in agreement with the Maberly et al. (1992) and Raven et al. (2002a) thresholds. So, macroalgae were classified into four strategies for DIC uptake: 1) CCM-only by active uptake HCO_3^- ($\delta^{13}C > -10$‰), 2) CCM active uptake HCO_3^- and/or diffusive uptake CO_2 ($\delta^{13}C < -11$ to -30‰), 3) Non-CCM, CO_2 by diffusion only ($\delta^{13}C < -30$‰), 4) Calcifying with different carbon-use strategies related to different modes of calcification. The measured δ^{13}C-macroalgal signals are integrative of the discrimination by photosynthesis ($\Delta^{13}C_p$) on the carbon source (δ^{13}C-DIC in seawater), respiration ($\Delta^{13}C_r$), and probable CO_2 leak out inside the cell during the CCM process (Sharkey and Berry, 1985; Raven et al., 2005; Carvalho et al., 2009a,b).

Macroalgae were grouped according to their characteristics morpho-functional proposed initially by Littler and Littler (1980) and modified by Balata et al. (2011). Most of the macroalgae species showed a limited distribution along the GC coastlines. Few cosmopolites' species included *Colpomenia tuberculata*, *Sargassum sinicola*, *Padina durvillei*, and *Ulva lactuca*. Also, not all morphofunctional groups and taxon were present in every site during each sampling survey, and the sample size in each group varied for taxa, location, and time.

A basic statistical analysis of δ^{13}C values in different macroalgae groups was applied to distribute and calculate the arithmetic mean, standard deviation, minimum and maximum. Because not all macroalgal species were present in sufficient numbers at different collection habitats, several macroalgal groups were not considered for statistical analysis. We compared among taxon and morphofunctional groups, collected in the same habitat (within-subjects factor) by multivariate analysis of variance. When differences were noted, a Tukey-Kramer HSD (Honestly Significant Difference) test was performed. Besides, variations of $\delta^{13}C$ macroalgal in specimens of the same morpho-functional and taxon collected in different habitats were also investigated with a Kruskal-Wallis test.

The relationships between $\delta^{13}C$ with each independent variable inherent to the macroalgae properties (taxon and morphology), biogeographical collection zone (GC coastline and coastal sector), habitat features (substrate, hydrodynamic, protection, and emersion level) and environmental conditions (temperature, pH, and salinity), were examined through simple and multiple linear regression analyses. Excepting temperature, pH, and salinity, most of the independent variables are categorical independent variables. However, these continue variables were also categorized, such as previously was described. Simple linear regression analyses were performed to establish the relationships between $\delta^{13}C$-macroalgal with each environmental parameter analyzed as possible driving factors (e.g., temperature, salinity, and pH). Multiple linear regression analyses were conducted to evaluate the combined effects of those independent variables (macroalgae properties, biogeographical collection zone, habitat features, and environmental conditions) on the $\delta^{13}C$-macroalgal. In the multivariable regression model, the dependent variable, $\delta^{13}C$-macroalgal, is described as a linear function of the independent variables X_i, as follows: $\delta^{13}C\text{-macroalgal} = a + b_1(X_1) + b_2(X_2) + \ldots + b_n(X_n)$ (1). Where a is regression constant (it is the value of intercept and its value is zero); b_1, b_2, and b_n, are regression coefficients for each independent variable X_i. From each one of the fitted regression models, we extracted the estimated regression coefficients for each of the predictor variables (e.g., Bayesian Information Criterion (BIC), Akaike Information Criterion (AIC), root-mean-square error (RMSE), Mallow's Cp criterion, F Ratio test, p-value for the test (Prob > F), coefficients of determination (R^2) and the adjusted R^2 statistics) (SAS Institute Inc., 2018). All regression coefficients were used as indicators of the quality of the regression (Draper and Smith, 1998; Burnham and Anderson, 2002). Kolmogorov-Smirnov normality test was applied for all variables, and all were normally distributed. Most of the $\delta^{13}C$ values in each group showed a normal distribution. For all statistical tests, a probability $P<0.05$ was used to determine statistical significance. The statistical analysis of the results was done using JMP 14.0 software (SAS Institute Inc.).

3. Results

3.1. Taxonomy and morpho-functional groups

Sampled specimens belong to three Phyla, 63 genera, and 170 species. The Phyla were identified as Chlorophyta (25%), Ochrophyta (22%), and Rhodophyta (53%). The most representative genus (and their species) were *Ulva* (*U. lactuca, U. lobata, U. flexuosa,* and *U. intestinalis*), *Codium* (*C. amplivesiculatum* and *C. simulans*), *Chaetomorpha* (*C. antenina*), *Padina* (*P. durvillei*), *Dictyota* (*D. dichotoma*), *Colpomenia* (*C. tuberculata* and *C. sinuosa*), *Sargassum* (*S. sinicola* and *S. horridum*), *Amphiroa* (*Amphiroa* spp.), *Spyridia* spp, *Polysiphonia* spp., *Gymnogongrus* spp., *Gracilaria* (*G. vermiculophylla, G. pacifica* and *G. crispata*), *Hypnea* (*H. pannosa* and *H. johnstonii*) *Grateloupia* (*G. filicina* and *G. versicolor*), and *Laurencia* (*L. papillosa* and *L. pacifica*). The endemic species included Chlorophyta *Codium amplivesiculatum*, Rhodophyta *Laurencia papillosa*, *Chondracanthus squarrulosa*, *Gracilaria spinigera,* and *G. subsecundata*, and Ochrophyta *Cutleria hancockii, Sargassum herphorizum, S. johnstonii*.

An analysis of the biogeographical diversity among sectors evidenced that P3 (43 genera of 63, 68%) and C3 (63%) at north recorded the highest number of the genus, followed by C1 (38%) and P1 (29%) at the south, and P2 (27%) and C2 (22%). The same pattern was observed in the species diversity, zones P3 (94 of 167 species, 56%) and C3 (52%) at the north, C1 (34%) and P1 (25%) at the south, and C2 and P2 (19-20%) at the center.

The morphofunctional groups identified were 21. The most common were C-tubular (6 spp., n=69; C-Blade-like (6 spp, n=55); C-Filamentous uniseriate (17 spp, n=49); C-Erect thallus (5 spp, n=33); O-Compressed with branched or divided thallus (19 spp., n=92); O-Thick leathery macrophytes (12 spp., n=104); O-Hollow with spherical or subspherical shape (4 spp, n=87); R-Large-sized corticated (57 spp., n=225); R-Filamentous uniseriate and pluriseriate with erect thallus (9 spp., n=48); and R-Large-sized articulated corallines (6 spp, n=17). The diversity, in terms of presence/absence of the morphofunctional groups, varied among coastline sectors, higher in C3 (16 of 21, 76%) and P3 (71%) at the north, followed by C1 (57%) and P1 (48%) at the south, and C2 and P2 and (42-48%) at the center of both GC coastlines.

3.2. δ^{13}C-macroalgal variability in function of taxonomy and morpho-functional groups

The variability of δ^{13}C values in macroalgae was analyzed by taxon (phylum, genus, species) and morphofunctional groups classified by habitat, coastal sector, and collection season. A complete list of the results of δ^{13}C in 170 macroalgae species is provided in Supporting Information (Table SI-1). Firstly, δ^{13}C values analyzed by phylum showed a unimodal distribution with a peak at -14±1.4‰ (Fig 2). Ochrophyta (-21.5 to -2.2‰, -12.5±3.7‰), displayed significantly higher values than Chlorophyta (-25.9 to -5.5‰, -14.5±3.0‰) and Rhodophyta (-34.6 to -4.5‰, -14.8±3.9‰). The δ^{13}C-macroalgal values (average±SD) for the genus of Chlorophyta, Ochrophyta, and Rhodophyta

(Fig. 3) varied from -33.8±1.1‰ for *Schizymenia* to -7.8±0.7‰ for *Amphiroa*. Based on the highest values, specimens of three Phyla showed δ^{13}C values>-10‰, evidenced the presence of CCM's by active uptake of HCO_3^- (strategy 1) (Fig. 3). For example, *Caulerpa, Cladophora, Codium, Ulva* for Chlorophyta *Colpomenia, Dictyota, Padina, Sargassum* for Ochrophyta, and *Hypnea* and *Polysiphonia* for Rhodophyta showed δ^{13}C values >-10‰. Likewise, high δ^{13}C values were observed in the calcifying macroalgae genus *Amphiroa* and *Jania*, under strategy 4 (Fig. 3c). δ^{13}C values lower than -30‰ that denote uptake of CO_2 by diffusion (strategy 3), were observed only in Rhodophyta *Schizymenia*, *Halymenia, and Gigartina*. However, most species showed large δ^{13}C variabilities that evidence a mechanism that uses a mix of HCO_3^- and CO_2 for photosynthesis (strategy 2).

Multiple comparison analyses revealed significant differences in the δ^{13}C-macroalgal values among genera, ordered as *Schizymenia* < *Polysiphonia* < *Ulva*, *Gracilaria* and *Spyridia* (-16.1±0.6‰ to -15.1±0.2‰) < *Gymnogongrus, Laurencia, Hypnea, Cladophora, Dictyota, Sargasumm, Chaetomorpha*, and *Grateloupia* (from -15.4±0.7‰ to -13.8±0.8‰) < *Codium* and *Padina* (-12.5±2.4‰ to -12.4±2.5‰) < *Colpomenia* and *Amphiroa* (-9.2±0.3 to -7.8±0.7‰) (F=16.81, p<0.001).

Aggrupation of δ^{13}C values based on morpho-functional features is displayed in Fig. 4. The most representative groups in the phylum Chlorophyta varied from -15.8±0.3‰ for C-Tubular to -12.4±0.5‰ for C-Thallus erect. The phylum Ochrophyta includes O-Thick leathery with the lowest mean (-14.8±0.3‰) and O-Hollow with a spherical or subspherical shape with the highest values (-9.2±0.3‰). The lowest and highest δ^{13}C values for Rhodophyta were observed for R-flattened macrophytes (-24.0±9.6‰) and R-Larger-sized articulated coralline (-7.89±0.75‰), respectively. Significant differences were observed among groups, which were ordered as follows: R-Flattened macrophytes < R-Blade like < C-Tubular < O-Tick leathery and R-Large size corticated < C-Blade like and C-Filamentous uniseriate < C- Thallus erect and O-Compressed with branch < O-Hollow with spherical < R-Larger-sized articulated coralline.

High intraspecific variability in $\delta^{13}C$ signal for the more representative genera of each taxon is showed in Table 1-3. For *Codium*, *C. brandegeei* (11.8±1.2‰) and *C. simulans* (-11.4±2.2‰) showed higher $\delta^{13}C$ values than *C. amplivesculatum* (-14.4±2.7‰). *Colpomenia* species had higher $\delta^{13}C$ values than the other genera, with higher values for *C. tuberculata* (-8.7±3.2‰) than *Colpomenia* sp. (-10.9±3.6‰) and *C. sinuosa* (-10.2±2.9‰). *Gracilaria* showed comparable $\delta^{13}C$ values in the four species (from -16.4±1.6‰ for *G. pacifica* to -15.5±2.4‰ for *Gracilaria* sp.). *Hypnea* showed non-significant $\delta^{13}C$ differences in three representative species (-16.4±1.7‰ for *H. spinella* to -14.9±2.3‰ for *Hypnea* sp.). *Laurencia* sp. (-12.9±1.2‰) was higher than *L. pacifica* (-14.9±2.2‰), while *Padina* sp. (-11.1±1.5‰) higher than *P. durvillei* (-13.2±2.6‰). *Sargassum* was one of the most diverse genera studied with six representative species, with $\delta^{13}C$ values ordered as follow: *S. horridum* = *S. sinicola* = *S. johnstonii* (-15.5±2.9 to -15.1±2.4‰) < *S. lapazeanum* (-14.5±1.6‰) = *Sargassum* sp. (-14.2±2.3‰) < *S. herphorizum* (-13.6±1.6‰). *Spyridia* sp. (-17.0±1.2‰) and *S. filamentosa* (-15.8±3.8‰) showed non-significant differences. The six representative species of *Ulva* were divided into two morphological groups, filamentous and laminates. Filamentous species that averaged -16.3±2.0‰ for *U. clathrata*, -16.0±3.6‰ for *U. flexuosa*, -15.7±1.7‰ for *U. acanthophora* and -15.3±2.5‰ for *U. intestinalis* and *Ulva* laminates that included *U. linza* (-15.5±2.4‰) and *U. lactuca* (-14.1±3.1‰). Non-significant differences were observed between morphological groups and among species. A high intra-specific variability, 11-28%, explains average overlapping.

3.3. $\delta^{13}C$-macroalgal variability in coastal sectors

A variety of macroalgal assemblages were documented along the GC coastlines, with differences in the taxonomic composition according to their fico-floristic region. Multiple comparison analysis of $\delta^{13}C$ signals evidenced significant differences between the most common genus and species of macroalgae between and within assemblages grouped by coastal sector, season and collecting year (Supplementary Information Tables SI-2-3). For example, genus *Padina* (e.g., *P. durvillei*) and *Ulva* (*e.g., U. lactuca*), collected in C1 sector during the rainy season, showed lower $\delta^{13}C$ values than in other sectors. Differences in the $\delta^{13}C$ signal are mainly related to the carbon uptake strategies of the macroalgae (Fig. 5). Even though most species inhabiting the GC coastal sectors displayed domination of strategies based on active CCM's, but the tendencies were different between taxa and coastal regions. The strategy 2 with mixing DIC sources are dominant in all regions and taxa (60-90%). Exceptions were observed in the P1 (68%) and C1 (37%) regions for Ochrophyta, where the specialized strategy 1 of only HCO_3^- user was significant. The strategy 3 based on the use of CO_2 was observed in the peninsular coast in P2 and P3 for Rhodophyta with 2-3.3%. Overall, more negative $\delta^{13}C$ values were observed at continental (C2) compared to the peninsular coastline (P1-P3) and southward than northward.

3.4. $\delta^{13}C$-macroalgal variability in function of taxonomy and habitat features and environmental conditions

Variability of $\delta^{13}C$ values for the most representative genera was evaluated by multiple comparative analyses in the habitat features' function, including the substrate, hydrodynamic, and emersion level. Large $\delta^{13}C$ variability observed between specimens of the same genus collected in the different habits do not show any significant pattern, and non-significant differences were observed. An exception was observed with the emersion level (showed in Fig. 6), where intertidal specimens recorded lesser negative values than subtidal in most macroalgae genus. For example, for

Hydroclathrus (intertidal -5.7±0.9‰; subtidal -11.4±5.9‰), *Amphiroa* (intertidal -6.9±1.5; subtidal -9.9±6.1), *Hypnea* (intertidal -13.5±2.5‰; subtidal -18.6±1.8‰), and *Laurencia* (intertidal -13.5±1.3‰; subtidal -17.1±1.8‰). Exceptions were observed for *Polysiphonia* (intertidal -19.7±2.2‰, subtidal -14.9±6.7‰), *Spyridia* (intertidal -16.9±3.3‰, subtidal -13.2±0.7‰) and *Colpomenia* (intertidal -9.4±3.4‰, subtidal -7.7±1.3‰).

Non-significant differences were observed for the same genera at different temperatures ranges, except for *Grateloupia* (cold, -19.2±4.7‰, typical -14.4±2.2‰, warm -14.5±2.2‰) and *Polysiphonia* (cold, -21.0±0.4‰, typical -18.1±5.5‰, warm -17.9±2.3‰) with more negative values in colder than warmer waters (F=6.42, p<0.001). Neither significant difference was observed in $\delta^{13}C$ values in macroalgae specimens from the different genus in the same temperature range (Fig. 7a).

Significant differences were observed among genus related to the pH level at seawater (Fig. 7b). Under typical pH seawater, *Amphiroa* and *Colpomenia* were 1-2‰ more negatives than in alkaline waters, while *Ulva* and *Spyridia* were 3-5‰ less negative than in acidic waters. *Amphiroa* and *Colpomenia* were not collected in acidic water, and neither *Spyridia* in alkaline waters to compare. Another genus also showed extremes values between alkaline (*Tacanoosca* -7.6±1.0‰) and acidic waters (*Schizymenia* -32.9±2.0‰). The following order was observed in the genus collect at the three pH ranges: alkaline > typical > acidic. Significant differences were observed for genus *Ahnfeltiopsis, Caulerpa, Gymnogongrus, Padina*, and *Ulva*, with higher values at alkaline than in acidic waters. Values of $\delta^{13}C$ for specimens of the same genus collected at typical pH waters are mostly overlapped between those for alkaline and acidic seawaters. Non-significant differences in $\delta^{13}C$ values were observed for *Grateloupia, Hypnea,* and *Polysiphonia* concerning pH-type waters.

We analyzed the carbon uptake strategies on macroalgal assemblages in the function of environmental factors like temperature, pH, and salinity (Fig. 8). Regarding the $\delta^{13}C$ variability for all data set in response to temperature and salinity, a non-significant trend was observed between $\delta^{13}C$-macroalgal in both parameters' function. A poor but significant correlation was observed between $\delta^{13}C$ and pH ($R^2 = 0.04$) (Table 4). The proportion of specimens with a strategy of only HCO_3^- use was different between environmental factors and taxa (previously described). For example, Ochrophyta showed the highest proportion (35%) in colder temperature, in pH-Alkaline (31%), and at typical salinity regimen (27%), while Chlorophyta enhanced to 30% in acid pH and Rhodophyta recorded 21% at normal seawater. The opposite strategy (only use of dissolved CO_2) was observed only in Rhodophyta. The highest percentage was observed in estuarine salinity regimen (10%).

3.5. Variation latitudinal of $\delta^{13}C$-macroalgal

The $\delta^{13}C$-macroalgal variation in the GC biogeography was evaluated by linear regression analysis between $\delta^{13}C$ values along the nine degrees latitude in both GC coastlines. A non-significant latitudinal trend was observed for datasets, but for the three Phyla's most representative genera, $\delta^{13}C$ values correlated with latitude (Fig. 9). In Chlorophyta, with the higher genera number, $\delta^{13}C$ values increased with latitude, with low but significant correlation. Contrarily, in Ochrophyta and Rhodophyta specimens, the $\delta^{13}C$ values decreased non-significantly with latitude.

In the most representative morphofunctional groups, significant correlations ($p<0.001$) were observed for $\delta^{13}C$-macroalgal *versus* latitude (Fig. 10). Representative morphofunctional groups of Chlorophyta (e.g., C-Tubular, C-Filamentous uniseriate), showed a positive correlation, while those belonging to Ochrophyta (e.g., O-Thick leathery;) and Rhodophyta (e.g., R-Large sized corticated) showed a negative trend with latitude.

3.6. Analyses of $\delta^{13}C$ macroalgal variability

An analysis of the effects, independent and combined, on the $\delta^{13}C$-macroalgal variability related to life form and environmental factors was conducted. Firstly, simple linear regression analyses were performed to evaluate the dependent variable's prediction power ($\delta^{13}C$-macroalgal) in the function of several independent variables controlling the main macroalgae photosynthesis drivers (light, DIC, and inorganic nutrients). Regression coefficients were estimated for each fitted regression model, which is used as indicators of the quality of the regression (Draper and Smith, 1998; Burnham and Anderson, 2002) as was described in Methods; however, our results description focused on the coefficients of determination (R^2 and adjusted R^2). The coefficient R^2 describes the overall relationship between the independent variables X_i with the dependent variable Y ($\delta^{13}C$-macroalgal), and it is interpreted as the % of contribution to the $\delta^{13}C$ variability. In comparison, the adjusted R^2 statistics compensate for possible confounding effects between variables.

Results of the analysis of the relationships between $\delta^{13}C$ with each independent variable are summarized in Table 4. Regarding the inherent macroalgae properties, Phyla explain only 8% variability, the morphofunctional properties 35%, genus 46%, and species 57%.

In terms of coastline (continental vs. peninsular) and coastal sectors (C1-C3 and P1-P3), the biogeographical collection zone explained a maximum of 5% variability. Only the emersion level (6%) contributed to the $\delta^{13}C$ variability related to the habitat features. The contribution of the seawater's environmental conditions was marginal for pH (4%) and negligible for temperature and salinity. A marginal reduction in the percentage of contribution was observed for Phyla (1%) and morphofunctional properties (1%), but significant for genus (5%) and species (10%).

Multiple regression analyses were also performed to interpret the complex relationships among $\delta^{13}C$-macroalgal, considering the life form (morphofunctional and taxon by genus) and their responses to environmental parameters. Results for the fitted regression models performed for morphofunctional groups (Table 5) and genus (Table 6) evidenced that the effect of the coastal sector and pH ranges on the δ^{13}C-macroalgal increased the contribution by 9-10% each one. The emersion level increased by 5-6%, the contribution respect to individual effect of morphofunctional group and genus, the temperature and pH in 1 and 3%, respectively, while salinity decreased by 1-2%. Adding the effect of the biogeographical collection zone, represented by the coastline sector, to those for morphofunctional group (Table 5) and genus (Table 7), a notable increase of 11-12% was observed. Considering the combined effect of the coastline sector + Habitats features for Morphofunctional group or Genus (Table 7), the full model showed R^2 of 0.60 and 0.71. In contrast, Coastline sector + Environmental conditions + Morphofunctional group or Genus the R^2 increased to 0.62 and 0.72, respectively. The interactive explanations of environmental factors increased the explanation percentage of δ^{13}C variability; however, these contributions were significantly lower than the explained by life forms, such as the morphofunctional properties and taxa by genus and species.

The combined effect of environmental conditions on the δ^{13}C variability was tested for the best-represented genus and morphological groups. Results evidenced that 9 of 21 morphological groups showed significant effects on the δ^{13}C variability (Table 8), five increasing and four decreasing the model constant of δ^{13}C=-14.2‰. For example, for the O-Hollow with spherical or subspherical shape (+4.9‰) and R-Larger-sized articulated corallines (+6.3‰), the predicted values are -7.9±0.8‰ and -9.2±0.4‰. For R-Filamentous uniseriate and pluriseriate with erect thallus (-2.1‰) and C-Tubular (-1.6‰), the predicted values are -16.3±0.5‰ and -15.8±0.5‰, respectively. Regarding taxon, a significant effect was observed only in 13 genera, including *Colpomenia* (+5.4‰), *Amphiroa* (+6.8‰), and *Padina* (+2.2‰) increasing the signal, and *Polysiphonia* (-3.7‰), *Gracilaria* (-0.9‰), and *Spyridia* (-1.4‰) decreasing the signal of the model constant (Table 9). In 33 species was observed a significant effect on the δ^{13}C variability, including *C. tuberculate* +5.9‰, *C. sinuosa*

+4.4‰, *H. pannosa* +4.4‰, *H. johnstonii* +4.4‰, and *Amphiroa spp*. (+4.4 to 8.2‰) increasing the model constant δ^{13}C= -14.6‰, and *Spyridia* sp. (-2.5‰), *G. filicina* (-2.3‰), *P. mollis* (-5.2‰) and *S. pacifica* (-19.2‰) (Table 10).

3.7. Preliminary estimations of Δ^{13}C-macroalgal

Concurrent analysis of surface seawater for alkalinity, proportions of the chemical species of DIC (CO_2, HCO_3^-, and CO_3^{2-}), and δ^{13}C-DIC evidenced that δ^{13}C-DIC in GC seawater averages 1.4±0.4‰ (-1 to 4.9‰) (Supplementary Information Fig. SI-1). In our preliminary data, the δ^{13}C-DICseawater slightly (in 0.5‰) decreased during the rainy season in those zones influenced by river discharges along the continental coastline. Non-significant differences were observed among coastal sectors. δ^{13}C-DIC values in GC seawater are comparable to the averages 1.4-1.6‰ reported for the surface seawaters in the Eastern North Pacific in the 1970s-2000s (Quay et al., 2003; Hinger et al., 2010; Santos et al., 2011).

Based on the subtraction of δ^{13}Cmacroalgae to δ^{13}C-DICseawater, the integrative discrimination factor against ^{13}C averaged 16.0±3.1‰, 16.8±4.3‰, and 14.0±3.8‰ for Phyla Chlorophyta, Rhodophyta, and Ochrophyta, respectively. Five groups were identified in the function of the Δ^{13}C values, one for Chlorophyta (Δ^{13}C=16.0±3.1‰), two for Rhodophyta (16.6±3.8‰ and 34.6±1‰), and two for Ochrophyta (9.1±1.7‰ and 15.7±2.7‰) (Fig. S2). Values of Δ^{13}C were comparable to δ^{13}C of the thallus of macroalgae. Thus, δ^{13}C-macroalgal reflect mainly the discrimination during carbon assimilation. Like δ^{13}C-macroalgal, the Δ^{13}C values were subject to considerable variation.

4. Discussions

4.1. Explaining the $\delta^{13}C$ macroalgal variability

This study revealed high variability in the $\delta^{13}C$ of the large inventory of macroalgae collected along GC coastline between five years period. A linear regression analysis of the effects of life forms revealed that the $\delta^{13}C$ variability in the -macroalgal community is mainly explained by taxonomic (genus 46%, species 57%) and morphofunctional groups. This result is consistent with the report of Lovelock et al. (2020), who found that 66% of $\delta^{13}C$ variability was explained by taxonomy. Even so, the variability associated with each genus is not the same and can be classified in three groups: 1) high variability (e.g., *Schizymenia* =±19.1‰), moderate variability (e.g., *Hydroclathrus*=±7.3‰; *Amphiroa* =±6.8‰) and low variability (e.g., *Gracilaria* =±0.89; *Spyridia* =±1.46‰). The observed $\delta^{13}C$ variability in this study is comparable with those reported in the literature, compiled in Table SI-4.

Most authors studying the isotopic composition of C in macroalgae have reported the high isotopic variability, which has been attributable to the taxon-specific photosynthetic DIC acquisition properties (Raven et al., 2002a, Mercado et al., 2009, Marconi et al., 2011, Stepien, 2015, Díaz-Pulido et al., 2016; Lovelock et al., 2020). Our study observed that the intrinsic characteristics of each morpho-functional group of macroalgae (e.g., thallus structure, growth form, branching pattern, and taxonomic affinities) also influence the $\delta^{13}C$-macroalgal signals. The thallus thickness, a morphology propriety, influences the diffusion boundary layer on the surface of the macroalgal, where they carry out the absorption of essential ions and dissolved gases (Hurd, 2000; San-Ford and Crawford, 2000). Thus, morphology can modulate the photosynthesis rates. However, a non-biological or ecological explanation of the $\delta^{13}C$ variability, and therefore carbon use physiology, can be given in terms of morphology.

The $\delta^{13}C$-macroalgal depends on the carbon source ($\delta^{13}C$-DIC in seawater), the isotope discrimination during carbon assimilation in the photosynthesis ($\Delta^{13}C_p$<29‰ in a variable degree), and the plant respiration ($\Delta^{13}C_r$ average ±2.3‰) (Carvalho et al., 2009a,b, 2010; Carvalho and Eyre, 2011, Rautenberger et al., 2015). Comparatively, the $\Delta^{13}C_r$ value is relatively small regarding $\Delta^{13}C_p$. Thus, $\delta^{13}C$-macroalgal is an integrative value of the isotope discrimination during DIC seawater assimilation [$\Delta^{13}C$= ($\delta^{13}C$-DIC seawater – $\delta^{13}C$macroalgae)] (Carvalho et al., 2009a). Based on the $\Delta^{13}C$ values, five groups were identified in our study: one for Chlorophyta ($\Delta^{13}C$=16.0±3.1‰), two for Rhodophyta (16.6±3.8‰ and 34.6±1‰), and two for Ochrophyta (9.1±1.7‰ and 15.7±2.7‰). Values of $\Delta^{13}C$ were comparable to $\delta^{13}C$ of the thallus of macroalgae. Thus, $\delta^{13}C$-macroalgal reflect mainly the discrimination during carbon assimilation. The $\delta^{13}C$-macroalgal values reflect the discrimination during carbon assimilation attributable to the taxon-specific photosynthetic DIC acquisition properties. $\Delta^{13}C$-macroalgal variability, captured in the $\delta^{13}C$-macroalgal signals, is related to the thickness of the boundary layer around the thallus (Raven et al. 1982), the leakage during carbon uptake (Sharkey and Berry 1985, Maberly et al. 1992), photosynthetic intensity (Wiencke and Fischer 1990, Kübler and Raven 1995, 1996), and respiration rates (Carvalho et al., 2010; Carvalho and Eyre, 2011, Rautenberger et al., 2015). All intrinsic properties are related to the life form.

Many species that recorded high $\delta^{13}C$ values (and low $\Delta^{13}C$ values) were fleshy macroalgae that are characterized to be bloom-forming macroalgae belonging to genera *Ulva, Gracilaria, Cladophora, Spyridia*, and *Sargassum* (Páez-Osuna et al., 2013, Valiela et al., 2018). It is not surprising that species with high photosynthetic activity and high relative growth rates (Hiraoka et al., 2020) have high carbon demand that results in lower isotopic discrimination against ^{13}C (Cornelisen, et al., 2007; Carvalho et al., 2010ab; Kübler and Dungeon, 2015; Rautenberger et al., 2015). Bloom-forming macroalgae (e.g., *Ulva, Gracilaria, Sargassum*) have been remarks as facultative species capable of switching from C3 to C4 pathway (Valiela et al., 2018). C4 pathway reduces photorespiration, the antagonist process of RuBisCo, enhancing the DIC assimilation in 25-40% and increasing the $\delta^{13}C$ values (Ehleringer et al., 1991; Bauwe et al., 2010; Zabaleta et al., 2012). C4 pathway has more energy investment in CCM's than in RuBisCo protein content than C3 pathway (Young et al., 2016). Also, the reports of C4 or C4-like pathway features in algae have increased in the last years (Roberts et al., 2007; Doubnerová and Ryslavá, 2011; Xu et al., 2012, 2013). For example, high activity of keys enzymes of C4 metabolisms, such as pyruvate orthophosphate dikinase (PPDK), phosphoenolpyruvate carboxylase (PEPC), and phosphoenolpyruvate carboxykinase (PCK), has been described in many algae species. But the establishment of a true C4 pathway in marine algae is not clear since the massive changes in gene expression patterns seem to be incomplete, and it is suggested that many marine algae have high plasticity to use a combination of CCM to overcome Ci limitations (Roberts et al., 2007; Doubnerová and Ryslavá, 2011; Xu et al.., 2012, 2013). A Stepwise model of the path from C3 to C4 photosynthesis is explained by Gowik and Westhoff (2011). More research is required on this topic considering the increasing the frequency, intensity, and extension of bloom-forming macroalgae events worldwide (Teichberg et al., 2010; Valiela et al., 2018) and in México (Ochoa-Izaguirre et al. 2007; Ochoa-Izaguirre and Soto-Jiménez 2015; Páez-Osuna et al., 2017).

Changes in the habitat features and environmental conditions, such as light intensity and DIC availability, influencing the growth rate and photosynthetic intensity, have a strong influence on $\delta^{13}C$ signal (Carvalho et al., 2007, 2009; Carvalho and Eyre, 2011; Stepien, 2015; Mackey et al., 2015; Rautenberger et al., 2015). The light intensity is the external factor with more influence on the $\Delta^{13}C$-macroalgal due to the regulation of carbon assimilation intensity (Wefer and Killingley 1986, Cooper and DeNiro 1989, Grice et al. 1996; Carvalho et al., 2009a,b). Experimental studies found the light levels as a key factor affecting the $\delta^{13}C$ values. For example, under saturating light conditions, *Ulva* switched from a carbon uptake of HCO_3^- and CO_2 to increased HCO_3^- use (Rautenberger et al., 2015). Furthermore, field studies have shown that species growing in low light habitats as deep subtidal tend to have more negative $\delta^{13}C$ values than those in higher light environments (Mercado et al., 2009; Hepburn et al., 2011; Marconi et al., 2011; Stepien 2015; Cornwall et al., 2015, Díaz-Pulido et al., 2016). In this study, intertidal specimens recorded lesser negative values than subtidal in most macroalgae genus. However, our study did not record the vertical effect in the $\delta^{13}C$ signal related to the light limitation because only shallow habitats (non-light limited) were studied.

$\delta^{13}C$-DICseawater is reasonably uniform in surface seawater (-4.8 to 3.6‰, median 1.5‰), with $\delta^{13}C$ values for CO_2, HCO_3^-, and CO_3^{2-} nearly -10, -0.5 and 2‰, respectively (Mook et al., 1974; Kroopnick, 1985). Exceptions can be expected where variations in the salinity, alkalinity, and proportions of the chemical species of DIC (CO_2, HCO_3^- or CO_3^{2-}) occur (e.g., in coastal environments influenced by river and groundwater discharges) (Mook et al., 1974; Chanton and Lewis 1999; Hinger et al., 2010; Carvalho et al., 2015). Regarding DIC sources for macroalgae in the GC surface seawater, the availability, chemical proportions, and $\delta^{13}C$-DIC, were also relatively constant and uniform. Thus, the influence of the $\delta^{13}C$-DIC variations on the $\delta^{13}C$-macroalgal variability is negligible in the GC.

The effect of other environmental factors, such as salinity and pH, on $\delta^{13}C$-macroalgal signals, were evaluated. Regarding salinity, the influence of freshwater discharge by rivers and groundwater decreases the $\delta^{13}C$ signal, which could be explained by the reduction in the salinity regimen that follows a decrease in $\delta^{13}C$-DIC in water (Hinger et al., 2010; Santos et al., 2011). In our study, a non-significant correlation between $\delta^{13}C$-macroalgal and salinity was observed.

Based on pH, differences in $\delta^{13}C$ were found only for a few genera (e.g., *Amphiroa, Colpomenia, Ulva, Spyridia*), with a trend to increase in the $\delta^{13}C$ values with pH increase, such as was reported by Maberly et al. (1992) and Raven et al. (2002b). Similar results were reported for Cornwall et al. (2017) in the field study, with the differential response of the $\delta^{13}C$ signals to pH among 19 species, in which only four species were sensitive to pH changes. A very weak but significant positive linear regression was observed between $\delta^{13}C$ and pH. Also, a trend to decrease in the $\delta^{13}C$ was recorded in the following order: alkaline > typical > acidic. According to Stepien (2015), the result of meta-analyzes between pH drift experiments and $\delta^{13}C$ thresholds was positive only for Rhodophyta and Ochrophyte but not for Chlorophyta. About 86% of the Stepien metadata met the theoretical CCM assignation based on both parameters, exceptions for species with $\delta^{13}C<-30‰$ that have been capable of raising $pH>9$. A strong association between pH compensation point and $\delta^{13}C$ was reported by Iñiguez et al. (2009) in three taxa of polar macroalgae. Environmental conditions may influence the $\delta^{13}C$-macroalgal values but not change the carbon use physiology in the macroalgae, which is most likely inherently species-specific.

4.2. Using $\delta^{13}C$-macroalgal to indicate the presence of an active CCM

In our study, the $\delta^{13}C$ signals from the thallus of macroalgae were used to evidence the presence of an active CCM. This tool was first used in macroalgal shallows communities of the Gulf of California. Most macroalgae species displayed $\delta^{13}C$ values that exhibit an active CCM's. Then, macroalgae were classified into four strategies for DIC uptake, in agreement with the Maberly et al. (1992) and Raven et al. (2002) thresholds: 1) CCM-only by active uptake HCO_3^- ($\delta^{13}C>-10‰$), 2) CCM active uptake HCO_3^- and/or diffusive uptake CO_2 ($\delta^{13}C<-11$ to $-30‰$), 3) Non-CCM, CO_2 by diffusion only ($\delta^{13}C<-30‰$), 4) Calcifying with different carbon-use strategies related to different modes of calcification. About of 84% of the total analyzed specimens showed the facultative uptake of HCO_3^- and CO_2, the most common strategy identified in macroalgal shallow communities (Hepburn et al., 2011; Cornwall et al., 2015; Stepien 2015; Díaz-Pulido et al., 2016). Based on the carbon uptake strategies, the most abundant macroalgae were those able to use both HCO_3^- and/or CO_2 by means of active uptake plus passive diffusion (strategy 2).

Macroalgae collected in GC also involved those that are only HCO_3^- users (strategy 1) and those relying on diffusive CO_2 uptake (strategy 3). Photosynthesis that relies on CO_2 uptake (lack of CMM), the most primitive mechanism (Cerling et al., 1993), has fewer energy costs than HCO_3^- uptake, which requires complex machinery with a high operational cost (Giordano et al., 2005; Hopkinson et al., 2011; Hopkinson, 2014; Raven and Beardall, 2016). The energy for macroalgae to uptake HCO_3^-, cross the plasma membrane, and covert to CO_2 for photosynthesis, is obtained through irradiance (Cornelisen et al., 2007). Based on our sampling effort, focused on intertidal and shallow subtidal habitats featured by high-light intensities, we expected high proportions of species with the carbon uptake strategy that uses only HCO_3^-. Results evidenced that strategy 1 was recorded in specimens belonging to 58 species of 170 total species. The higher proportions of CCM species (HCO_3^- users) with high-energetic requirements are explained by those elevated irradiances (Hepburn et al. 2011; Cornwall et al. 2015). Ochrophyta showed the highest proportion of species that depend only on HCO_3^- uptake on both coastlines in the southern region of GC (P1, C1). Low solubility of CO_2 is related to high temperatures in subtropical waters (Zeebe and Wolf-Gladrow, 2007) that impulse the development of CCM (Raven et al., 2002b) and by the high affinity to DIC by Ochrophyta, such as has been described before by Diaz-Pulido et al, (2016).

Only three non-calcifying species (*Schizymenia pacifica*, *Halymenia* sp., *Gigartina* sp.) belonging to Rhodophyta were CO_2 exclusive users ($\delta^{13}C=-33.2\pm1‰$). Based on measurements of pH drift, Murru and Sandgreen (2004) reported *Schizymenia pacifica* and two species of Halymenia (e.g., *H.*

schizymenioides and H. gardner) as restricted CO_2 users. Measurements of $\delta^{13}C$ in *Halymenia dilatate* confirmed the CO_2-restricted photosynthesis in specimens collected offshore in deep reefs of the Great Barrier reef (Díaz-Pulido et al., 2016). Red macroalgae that lack CCM, tend to inhabit low-light habitats like subtidal or low intertidal and are abundant in cold waters (Kübler et al., 1999; Raven et al., 2002a; Cornwall et al., 2015). According to these authors, approximately 35% of the total red algae tested globally are strictly CO_2 dependents. The percentage of macroalgae species representative of Arctic and Antarctic ecosystems that lack CCM is 42-60% (Raven et al., 2002b; Iñiguez et al., 2019), 50% for temperate waters of New Zealand (Hepburn et al., 2011), and up to 90% found for a single site of Tazmania, Australia (Cornwall et al., 2015). Our study sampled 91 red macroalgae species (of 453 red macroalgae species reported in the GC, Pedroche and Sentíes, 2003), of which <3% were CO_2 dependents. This low percentage could be related to the fact that deep habitats (>2 m depth low tide) were not explored in our surveys.

Few calcifying macroalgae species using HCO_3^- and CO_2 (strategy 4) were also collected, including the genera *Amphiroa* (-7.8±3.7‰) and *Jania* (-9.4±0.7‰), both Rhodophyta with articulated-form. *Padina*, a genus with less capacity to precipitate $CaCO_3$ (Ilus et al., 2017), displayed relatively high $\delta^{13}C$ values (-12.5±2.4‰), suggesting the presence of CCM using HCO_3^-. Some species of *Padina* can use HCO_3^-, but their efficiency may differ from species to species (Raven et al., 2002a; Enríquez and Rodríguez-Román, 2006). Three genera are widespread in the GC. Stepien (2015) reported a global mean of -14.8±1.0‰ for calcifying species compared to -20.1±0.3‰ for non-calcifying species. Calcifying species have a different carbon uptake strategy influenced by the calcifying process that results in elevated $\delta^{13}C$ signals (Diaz-Pulido et al., 2016). One possibility for high $\delta^{13}C$ values for calcifying species are related to the excess of H^+ released as residuals products of the calcifying process. Also, the acidified boundary layers benefit the HCO_3^- uptake (McConnaughey and Whelan 1997, Courneau et al., 2012). Another possibility to explain high $\delta^{13}C$ values can also be related to the highly efficient light properties enhanced by the carbonate skeleton, resulting in an optimization of photosynthetic activity (Vásquez-Elizondo et al., 2017). Hofmann and Heesch (2018) reported high $\delta^{13}C$ values in eight rhodoliths species (calcifying species) for the organic matter thallus and for thallus, including $CaCO_3$ structure collected in deep habitats (25-40 m) where light availability is limited. Because the ocean acidification in progress, negative impacts are expected on calcifying organisms, more attention as ecological sentinels is warranted in the GC.

Measurements of $\delta^{13}C$ signals evidence the presence or absence of CCMs in macroalgae and are indicative of carbon use physiology (Giordano et al., 2005), however, the isotopic signature may be inconclusive in the determination of the efficient use of one or more DIC species (CO_2 and/or HCO_3^-) (Roleda and Hurd, 2012). The preferential DIC uptake of macroalgae is assessed by pH drift experiments (Hepburn et al., 2011; Roleda and Hurd, 2012; Fernandez et al. 2014, 2015; Narvarte et al., 2020) and it can be determined by simultaneously measuring the CO_2 uptake and O_2 production rates using membrane-inlet mass spectroscopy (MIMS) (Douchi et al., 2019; Burlacot et al., 2020). Macroalgae that are unable to raise the seawater pH>9.0 are primarily CO_2-users, while those that can raise the seawater pH>9.0 (absence of CO_2) are HCO_3^--users (Roleda; Hurd, 2012). Those differences in the carbon uptake strategies can be easily deduced by pH drift experiments, which were not done in our study but reported in the literature (Supplementary Information Table SI-4). Also, the change in $\delta^{13}C$ signature within the range specific to a carbon use strategy (e.g., mix HCO_3/CO_2^--user) can be complemented by simultaneous measurements of O_2 and CO_2 produced and consumed, respectively, during the photosynthetic using MIMS. For example, photosynthetic O_2 production in a certain macroalgae species with an active CCM preferring (e.g., CO_2) is about ten times higher than no active CCM (Burlacot et al., 2020).

Based on the $\delta^{13}C$ values, it is possible to assume that at least one basal CCM is active, however, it is impossible to discern what type of CCM is expressed in the organisms (e.g., direct HCO_3^- uptake by the anion-exchange protein AE; Drechsler and Beer 1991; Drechsler et al. 1993) or types of mitochondrial carbonic anhydrase (e.g., internal and external) that enhance the fixation of Ci by recycling mitochondrial CO_2 (Bowes, 1969; Zabaleta et al., 2012; Jensen et al., 2020). Also, the co-existence of different CCMs has been described for the same species (Axelsson et al., 1999, Xu et al., 2012), even that different CCM's can operate simultaneously, generating different Ci contributions to RuBisCo internal pool (Rautenberger et al., 2015). The variety of CCMs and their combinations could contribute to the high $\delta^{13}C$ variability for the same species. In our field study, it is impossible to explain the variations of $\delta^{13}C$ or $\Delta^{13}C$-macroalgal relative to CCM or CA activity types. Controlled experiments, like those conducted by Carvalho and collaborators (e.g., Carvalho et al. 2009a,b, 2010), are required to obtain this knowledge.

4.3. Variability of $\delta^{13}C$ macroalgal between the GC bioregions

Changes in the $\delta^{13}C$ signal with latitude, mainly related to the light and temperature, have been reported in the literature (Mercado et al., 2009; Marconi et al., 2011; Stepien, 2015; Hofmann and Heesch, 2018; Lovelock et al., 2020). For example, a negative correlation between latitude and $\delta^{13}C$-macroalgal was described by Stepien (2015), concluding that the $\delta^{13}C$ signal increased by 0.09‰ for each latitude degree from the Equator. Hofmann and Heesch (2018) recently showed a strong decrease in latitudinal effect (R^2= 0.43 $\delta^{13}C_{total}$ and 0.13, for $\delta^{13}C_{organic\text{-}tissue}$, p=0.001) for rhodolite of the northern hemisphere and macroalgae from coral reefs in Australia. In both cases, the latitude range is higher than we tested (30º to 80º and from 10º to 45º, respectively). These differences on a big scale tend to be associated with a temperature effect (Stepien, 2015) and their effect on CO_2 solubility in seawater (Zeebe and Wolf-Gladrow, 2007). However, in our study, any geographical pattern in the $\delta^{13}C$ macroalgal was observed. Our linear regression analyzes for latitudes showed a low but significant correlation for the dataset classified by morphofunctional groups and genus, negative in the cases of Rhodophyta and Ochrophyta groups, and positive for Chlorophyta.

Light is not limited along the GC latitudes. Most of the shallow habitats occupied by macroalgal communities in the GC were high-light environments. In agreement to literature, the surface seawater temperature across the GC vary in only 1ºC annual mean (Escalante et al., 2013, Robles-Tamayo, 2018). However, larger temperature variations of 5-10ºC were recorded in the coastal waters across the GC bioregions in both climatic seasons. The combined effect of the coastline sector, habitats feature, or environmental condition for Morphofunctional group or Genus explained 60-62 and 71-72% of the $\delta^{13}C$ variability, respectively. Our analysis of variability for the best-represented morphological groups (e.g., R-Filamentous uniseriate and pluriseriate with erect thallus and C-Tubular) and genus (e.g., *Colpomenia*, *Padina*, *Polysiphonia* and *Gracilaria*) revealed that certain life forms are better monitors explaining the variability of $\delta^{13}C$-macroalgal (and $\Delta^{13}C$ values) than others. The $\delta^{13}C$ variability in morphological groups refers to change within a specific carbon use strategy, but not change in the carbon use physiology that is inherently species-specific. The biological or ecological relevance of the $\delta^{13}C$ variability in function of the morphology, in terms of the efficiency in the use of DIC and the isotope discrimination during carbon assimilation and respiration, must be investigated in species of same genus morphologically different or between same morphological structures belonging to a different taxon.

The proportion of specimens with different carbon uptake strategies also showed regional variations. For example, the facultative uptake of HCO_3^- and CO_2 was dominant in the macroalgal shallow communities in the GC (60 to 90% of specimens), with an exception in the P1 region for Ochrophyta where the specialized strategy of only HCO_3^- use dominated (68%), and high proportion were observed in C1 with 37%. While the strategy based on only use of CO_2 was observed in the peninsular coast in P2 and P3 for Rhodophyta with 2-3.3%. Finally, the coastal sector C2 showed more negative $\delta^{13}C$ values in macroalgae specimens of the same genus compared to the peninsular coastline (P1-P3). Small but detectable changes were observed in the Phyla distribution based on environmental conditions. For example, Ochrophyta showed the highest proportion (35%) in colder temperature, in pH-Alkaline (31%), and at typical salinity regimen (27%), while Chlorophyta enhanced to 30% in acid pH and Rhodophyta recorded 21% at normal seawater. The opposite strategy (only use of dissolved CO_2) was observed only in Rhodophyta. The highest percentage was observed in the estuarine salinity regimen (10%). Again, more research is required to obtain valuable information on the physiological and environmental status of macroalgae.

5. Conclusions

In conclusion, we observed high $\delta^{13}C$-macroalgal variability in macroalgae communities in the Gulf of California, such as reported in other worldwide marine ecosystems. The life form is the principal cause of $\delta^{13}C$-macroalgal variability, which explains up to 57% of the variability. Changes in habitat characteristics and environmental conditions also influence the $\delta^{13}C$-macroalgal variability within a specific carbon use strategy. Considering the combined effect of the life form, coastline sector, and environmental conditions, the full model explains up to 72% (genus) of the variability. The effect of the coastal sector, pH ranges, and emersion level were significant, while for salinity and temperature, negligible.

Most macroalgae inhabiting in GC displayed the presence of CO_2 concentrating mechanisms to uptake HCO_3^- for photosynthesis, 84% of the total analyzed specimens were able to use both HCO_3^-

and/or CO_2 employing active uptake plus passive diffusion (strategy 2: $-10<\delta^{13}C>-30‰$). Specimens belonging to 58 species of 170 total species showed carbon uptake strategy 1 that use only HCO_3^-. A higher proportion of CCM species (HCO_3^- users) was expected because we focused on intertidal and shallow subtidal habitats featured by high-light intensities. Only three non-calcifying species (*Schizymenia pacifica*, *Halymenia* sp., *Gigartina* sp.) belonging to Rhodophyta (3%) were CO2 exclusive users (strategy 3: $\delta^{13}C<-30‰$). The low percentage of CO_2 dependents versus 40-90% reported for temperate regions could be related to the shallow habitat sampled in our surveys (<2 m depth low tide). The calcifying macroalgae genera *Amphiroa* and *Jania* using HCO_3^- and diffusive CO_2 influenced by the calcification process (strategy 4) were present in the macroalgal communities along the GC and high $\delta^{13}C$ values. Because the ongoing ocean acidification, these calcifying organisms constitute excellent ecological sentinels in the GC.

Finally, diverse authors have reported significant correlations between $\delta^{13}C$ signal and latitude, mainly related to the light and temperature. However, in our study´s latitude range (21º-31ºN), the linear regression analyzes showed a low correlation for the $\delta^{13}C$-macroalgal dataset classified by morphofunctional groups and genus, being negative for Rhodophyta and Ochrophyta and positive for Chlorophyta. Non-clear $\delta^{13}C$-macroalgal patterns occur along the GC latitudes. However, detectable changes were observed in the $\delta^{13}C$-macroalgal and the proportion of specimens with different carbon uptake strategies among coastal sectors. For example, the facultative uptake of HCO_3^- and CO_2 was dominant in the macroalgal shallow communities in the GC (60 to 90% of specimens), but in the coastal sector P1 was the specialized strategy of only HCO_3^- use the dominant strategy (68%), and significant at C1 (37%).

Our research is the first approximation to understand the $\delta^{13}C$-macroalgal variability in one of the most diverse marine ecosystems in the world, the Gulf of California. We did not pretend to resolve the intricate processes controlling the variations of $\delta^{13}C$ or $\Delta^{13}C$-macroalgal during carbon assimilation and respiration and determine the isolated influence of each environmental factor. Despite the large dataset and corresponding statistical analyses, our study faces limitations due to research design and because no research on $\delta^{13}C$-macroalgal analysis was developed previously in the GC. The primary deficiency is the lack of pH drift experiments to discriminate $\delta^{13}C$ signal variations to the carbon uptake strategies to determine preferential DIC uptake of macroalgae (CO_2 or HCO_3^-). The second limitation concerns the lack of controlled experiments to discern what type of CCM is expressed in macroalgae (e.g., direct HCO_3^- uptake by the anion-exchange protein AE, types of mitochondrial AC, or the co-existence of different CCMs). Also, more research is required to assess the biological or ecological relevance of the $\delta^{13}C$ variability in function of the morphology (e.g., DIC uptake efficiency and isotope discrimination during carbon assimilation and respiration). Future studies assessing the ability of macroalgae to use CO_2 and/or HCO_3^- can be assessed by pH drift experiments and/or MIMS in the cosmopolites' species and within of genus with differences in the $\delta^{13}C$ values between species (e.g., *Ulva* and *Sargassum*). Finally, controlled experiments in laboratory and mesocosm type combined with field studies are required to elucidate what type of CCM is expressed in macroalgae. Even so, the $\delta^{13}C$-macroalgal was a good indicator to infer the presence or absence of CCM's and identify the macroalgae lineages that could be in a competitive advantage based on their carbon uptake strategy and identify their geographical distribution along with GC. Under the current conditions of climate change and their effects as ocean acidification progresses and the bloom-forming macroalgae events increase in México and worldwide, the analysis of $\delta^{13}C$-macroalgal constitutes an excellent tool to help to predict the prevalence and shift of species in macroalgal communities' focused on carbon metabolism. However, to obtain the maximum benefit from isotopic tools in the carbon-use strategies study, diverse and species-specific, it is necessary to use them in combination with other techniques referred to herein.

6. Data Availability Statement

Data set are each permanently deposited Soto-Jimenez, Martin F; Velázquez-Ochoa, Roberto; Ochoa Izaguirre, Maria Julia. Earth and Space Science Open Archive ESSOAr; Washington, Nov 25, 2020. DOI:10.1002/essoar.10504972.1

https://search.proquest.com/openview/2060de58b217ca47495469b53ae2f347/1?pq-origsite=gscholar&cbl=4882998

7. Author contribution

Velázquez-Ochoa R. participate in the collection, processing, and analysis of the samples as a part of his master's degree thesis. Ochoa-Izaguirre J. also participate in sample collections and identified macroalgae specimens. Soto-Jiménez M.F. coordinated the research, was the graduate thesis director and prepared the manuscript with contributions from all co-authors.

8. Competing interests

The authors declare that they have no conflict of interest.

9. Acknowledgements

The authors would like to thank H. Bojórquez-Leyva, Y. Montaño-Ley, and A. Cruz-López for their invaluable field and laboratory work assistance. Thanks to S. Soto Morales for the English revision. UNAM-PAPIIT IN206409 and IN208613 provided financial support, and UNAM-PASPA supported MF Soto-Jimenez for Sabbatical year.

10. References

Abbot, I. A., and Hollenberg, G.: Marine algae of California. Standford University Press, California.

1976.

Aguilar-Rosas, L. E., and R. Aguilar-Rosas, R.: Ficogeografía de las algas pardas (Phaeophyta) de la península de Baja California, in: Biodiversidad Marina y Costera de México (Comisión Nacional Biodiversidad y CIQRO, México), edited by: Salazar-Vallejo, S. I. and González, N. E., 197-206, 1993.

Aguilar-Rosas, L. E., Pedroche, F. F., and Zertuche-González, J. A.: Algas Marinas no nativas en la costa del Pacífico Mexicano. Especies acuáticas invasoras en México. Comisión Nacional para el Conocimiento y Uso de la Biodiversidad, México, 211-222, 2014.

Álvarez-Borrego, S.: Gulf of California., in: Ecosystems of the World, 26. *Estuaries and Enclosed Seas,* (Elsevier, Amsterdam), Edited by: Ketchum BH., 427–449, 1983.

Anthony, K. R., Ridd, P. V., Orpin, A. R., Larcombe, P., and Lough, J.: Temporal variation of light availability in coastal benthic habitats: Effects of clouds, turbidity, and tides, Limnol. Oceanogr., 49(6), 2201-2211, https://doi.org/10.4319/lo.2004.49.6.2201, 2004.

Axelsson, L., Larsson, C., and Ryberg, H.: Affinity, capacity and oxygen sensitivity of two different mechanisms for bicarbonate utilization in *Ulva lactuca* L. (Chlorophyta), Plant Cell Environ., 22, 969–978, https://doi.org/10.1046/j.1365-3040.1999.00470.x, 1999.

Balata, D., Piazzi, L., and Rindi, F.: Testing a new classification of morphological functional groups of marine macroalgae for the detection of responses to stress, Mar. Biol., 158, 2459–2469, https://doi.org/10.1007/s00227-011-1747-y, 2011.

Bastidas-Salamanca, M., Gonzalez-Silvera, A., Millán-Núñez, R., Santamaria-del-Angel, E., and Frouin, R.: Bio-optical characteristics of the Northern Gulf of California during June 2008, Int. J. Oceanogra., https://doi.org/10.1155/2014/384618, 2014.

Bauwe, H., Hagemann, M., and Fernie, A. R.: Photorespiration: players, partners and origin, Trends Plant Sci., 15(6), 330–336, https://doi.org/10.1016/j.tplants.2010.03.006, 2010.

Beardall, J., and Giordano, M.: Ecological implications of microalgal and cyanobacterial CO_2 concentrating mechanisms, and their regulation, Funct. Plant Biol., 29(3), 335–347, https://doi.org/10.1071/PP01195, 2002.

Bold, C. H., and Wynne, J. M.: Introduction to the Algae: Structure and reproduction. Prentice-Hall, Incorporated, 1978.

Bowes, G. W.: Carbonic anhydrase in marine algae, Plant Physiol., 44:726–732, https://doi.org/10.1104/pp.44.5.726, 1969.

Bray, N. A.: Thermohaline circulation in the Gulf of California, *J. Geophys. Res. Oceans.*, 93(C5), 4993–5020, https://doi.org/10.1029/JC093iC05p04993, 1988.

Brodeur, J. R., Chen, B., Su, J., Xu, Y. Y., Hussain, N., Scaboo, K. M., Zhang, Y., Testa, J. M. and Cai, W. J.: Chesapeake Bay inorganic carbon: Spatial distribution and seasonal variability, Front. Mar. Sci., https://doi.org/10.3389/fmars.2019.000996, 99, 2019.

Brusca, R. C., Findley, L. T., Hastings, P. A., Hendrickx, M. E., Cosio, J. T., and van der Heiden, A. M.: Macrofaunal diversity in the Gulf of California. Biodiversity, ecosystems, and conservation in Northern Mexico, 179, 2005.Burlacot, A., Burlacot, F., Li-Beisson, Y., and Peltier, G. (2020). Membrane inlet mass spectrometry: a powerful tool for algal research. Front. Plant Sci., 11, 1302. https://doi.org/10.3389/fpls.2020.01302, 2020.

Burlacot, A., Burlacot, F., Li-Beisson, Y., and Peltier, G.: Membrane inlet mass spectrometry: a powerful tool for algal research, Front. Plant Sci., 11, 1302, https://doi.org/10.3389/fmicb.2019.01356, 2020.

Burnham, K. P., and Anderson, D. R.: A practical information-theoretic approach, Model selection and multimodel inference, 2nd ed. Springer, New York, 2. 2002.

Carrillo, L., and Palacios-Hernández, E.: Seasonal evolution of the geostrophic circulation in the northern Gulf of California, Estuar. Coast. Shelf Sci., 54(2), 157–173, https://doi.org/10.1006/ecss.2001.0845, 2002.

Carvalho, M. C. and Eyre, B. D.: Carbon stable isotope discrimination during respiration in three seaweed species, Mar. Ecol. Prog. Ser., 437:41–49. https://doi.org/10.3354/meps09300, 2011.

Carvalho, M. C., Hayashizaki, K., Ogawa, H., and Kado, R.: Preliminary evidence of growth influence on carbon stable isotope composition of *Undaria pinnatifida,* Mar. Res. Indones., 32, 185-188, 2007.

Carvalho, M. C., Hayashizaki, K., and Ogawa, H.: Carbon stable isotope discrimination: a possible growth index for the kelp Undaria pinnatifida, Mar. Ecol. Prog. Ser., 381, 71-82, https://doi.org/10.3354/meps07948, 2009a.

Carvalho, M. C., Hayashizaki, K. I., and Ogawa, H.: Short-term measurement of carbon stable isotope discrimination in photosynthesis and respiration by aquatic macrophytes, with marine macroalgal examples, J. Phycol., 45(3), 761-770, 2009b.

Carvalho, M. C., Hayashizaki, K., and Ogawa, H.: Effect of pH on the carbon stable isotope fractionation in photosynthesis by the kelp *Undaria pinnatifida*, Coast. Mar. Sci, 34(1), 135-139, 2010a.

Carvalho, M. C., Hayashizaki, K., and Ogawa, H.: Temperature effect on carbon isotopic discrimination by *Undaria pinnatifida* (Phaeophyta) in a closed experimental system[1], J. Phycol, 46(6), 1180-1186, https://doi.org/10.1111/j.1529-8817.2010.00895.x, 2010b.

Carvalho, M. C., Santos, I. R., Maher, D. T., Cyronak, T., McMahon, A., Schulz, K. G., and Eyre, B. D.: Drivers of carbon isotopic fractionation in a coral reef lagoon: Predominance of demand over supply. Geoch. Cosmoch. Acta, 153, 105-115, https://doi.org/10.1016/j.gca.2015.01.012, 2015.

Cerling, T. E., Wang, Y., and Quade, J.: Expansion of C4 ecosystems as an indicator of global ecological change in the late Miocene, *Nature*, 361 (6410), 344–345, https://doi.org/10.1038/361344a0, 1993.

Chanton, J. P., and Lewis, F. G.: Plankton and dissolved inorganic carbon isotopic composition in a river-dominated estuary: Apalachicola Bay, Florida. Estuaries, 22(3), 575-583, https://doi.org/10.2307/1353045, 1999.

CNA (Comisión Nacional del Agua): Atlas del agua en México, 2012.

Comeau, S., Carpenter, R. C., and Edmunds, P. J.: Coral reef calcifiers buffer their response to ocean acidification using both bicarbonate and carbonate, *Proc. Bio. Sci.,* 280(1753), 20122374, https://doi.org/10.1098/rspb.2012.2374, 2012.

Cornelisen, C. D., Wing, S. R., Clark, K. L., Hamish Bowman, M., Frew, R. D., and Hurd, C. L.: Patterns in the δ^{13}C and δ^{15}N signature of *Ulva pertusa:* interaction between physical gradients and nutrient source pools, Limnol. Oceanogr, 52(2), 820-832, 2007.

Cornwall, C. E., Revill, A. T., and Hurd, C. L.: High prevalence of diffusive uptake of CO_2 by macroalgae in a temperate subtidal ecosystem, Photosynth. Res., 124, 181–190, https://doi.org/10.1007/s11120-015-0114-0, 2015.

Dawson, E. Y.: The marine algae of the Gulf of California, Allan Hancock Pac. Exped., 3(10), [i-v+] 189–453, 1944.

Dawson, E. Y.: Marine red algae of Pacific México. Part 2. *Cryptonemiales* (cont.), Allan Hancock Pac. Exped., 17(2), 241–397, 1954.

Dawson, E. Y.: How to know the seaweeds, Dubuque, Iowa, USA. W.M.C. Brown. Co. Publishers. pp 197., 1956.

Dawson, E. Y.: The marine red algae of Pacific Mexico, Part 4, Gigartinales. Allan Hancock Pacific Exped., 2, 191-343, 1961.

Dawson, E. Y.: Marine red algae of Pacific México. Part 7. *Ceramiales*: Ceramiaceae, Delesseriaceae, Allan Hancock Pac. Exped., 26(1), 1–207, 1962.

Dawson, E. Y.: Marine red algae of Pacific México. Part 8. *Ceramiales*: Dasyaceae, Rhodomelaceae. Nova Hedwigia, 6, 437–476, 1963.

Díaz-Pulido, G., Cornwall, C., Gartrell, P., Hurd, C., and Tran, D. V.: Strategies of dissolved inorganic carbon use in macroalgae across a gradient of terrestrial influence: implications for the Great Barrier Reef in the context of ocean acidification, Coral Reefs, 35(4), 1327-1341, https://doi.org/10.1007/s00338-016-1481-5 2016.Douchi, D., Liang, F., Cano, M., Xiong, W., Wang, B., Maness, P.C., Lindblad, P., Yu, J. Membrane-Inlet Mass Spectrometry enables a quantitative understanding of inorganic carbon uptake flux and carbon concentrating mechanisms in metabolically engineered cyanobacteria. Front. Microbiol. 10, 1356–1356. doi: 10.3389/fmicb.2019.01356, 2019.

Doubnerová, V., and Ryšlavá, H.: What can enzymes of C4 photosynthesis do for C3 plants under stress?, *Plant Sci.*, 180(4), 575–583, https://doi.org/10.1016/j.plantsci.2010.12.005, 2011.

Draper, N. R., and Smith, H.: Applied regression analysis, edited by: John Wiley & Sons (Vol. 326), 1998.

Drechsler, Z., and Beer, S.: Utilization of inorganic carbon by *Ulva lactuca*. *Plant Physiol.,* 97, 1439–1444, https://doi.org/10.1104/pp.97.4.1439, 1991.

Drechsler, Z., Sharkia, R., Cabantchik, Z. I., and Beer, S. Bicarbonate uptake in the marine macroalga *Ulva* sp. is inhibited by classical probes of anion exchange by red blood cells, *Planta*, 191(1), 34–40, https://doi.org/10.1007/BF00240893, 1993.

Dreckmann, K. M.: El género *Gracilaria* (Gracilariaceae, Rhodophyta) en el Pacífico centro-sur mexicano, Monografías ficológicas, 1, 77-118, 2002.

Dudgeon, S. R., Davison, I. R., and Vadas, R. L. Freezing tolerance in the intertidal red algae *Chondrus crispus* and *Mastocarpus stellatus:* Relative importance of acclimation and adaptation, Mar Biol., 106(3), 427–436, https://doi.org/10.1007/BF01344323, 1990.

Dudley, B. D., Barr, N. G., and Shima, J. S.: Influence of light intensity and nutrient source on δ^{13}C and δ^{15}N signatures in *Ulva pertusa,* Aquat. Biol., 9(1), 85–93, https://doi.org/10.3354/AB00241, 2010.

Ehleringer, J. R., Sage, R. F., Flanagan, L. B., and Pearcy, R. W.: Climate change and the evolution of C4 photosynthesis, Trends Ecol. Evol.*,* 6(3), 95–99, https://doi.org/10.1073/pnas.1718988115, 1991.

Enríquez, S., and Rodríguez-Román, A.: Effect of water flow on the photosynthesis of three marine macrophytes from a fringing-reef lagoon, *Mar. Ecol. Prog. Ser.*, 323, 119–132, https://doi.org/10.3354/meps323119, 2006.

Escalante, F., Valdez-Holguín, J. E., Álvarez-Borrego, S., and Lara-Lara, J. R.: Temporal and spatial variation of sea surface temperature, chlorophyll a, and primary productivity in the Gulf of California. Ciencias Marinas, 39(2), 203-215, 2013.

Espinoza-Avalos, J.: Macroalgas marinas del Golfo de California, Biodiversidad marina y costera de México (CONABIO- CIQRO, México), edited by: Salazar-Vallejo, S.I., González, N. E., 328–357, 1993.

Espinosa-Carreón, T. L., and Valdez-Holguín, E.: Variabilidad interanual de clorofila en el Golfo de California. Ecol. Apl., 6(1-2), 83–92, 2007.

Espinosa-Carreón, T. L., and Escobedo-Urías, D.: South region of the Gulf of California large marine ecosystem upwelling, fluxes of CO_2 and nutrients, Environ Dev., 22, 42–51, https://doi.org/10.1016/j.envdev.2017.03.005, 2017.

Fernández, P. A., Hurd, C. L., and Roleda, M. Y.: Bicarbonate uptake via an anion exchange protein is the main mechanism of inorganic carbon acquisition by the giant kelp *Macrocystis pyrifera* (L aminariales, Phaeophyceae) under variable pH, J. Phycol., 50(6), 998-1008, doi: 10.1111/jpy.12247., 2014.

Fernández, P. A., Roleda, M. Y., and Hurd, C. L., Effects of ocean acidification on the photosynthetic performance, carbonic anhydrase activity and growth of the giant kelp *Macrocystis pyrifera*, Photosynth. Res., 124(3), 293-304, 2015.

Gateau, H., Solymosi, K., Marchand, J., and Schoefs, B.: Carotenoids of microalgae used in food industry and medicine. Mini-Rev. Med. Chem., 17(13), 1140–1172, https://doi.org/10.2174/1389557516666160808123841, 2017.

Gilbert, J. Y., and Allen, W. E.: The phytoplankton of the Gulf of California obtained by the ‘‘E.W. Scripps’’ in 1939 and 1940, J. Mar. Res., 5, 89–110, https://doi.org/10.1016/0022-0981(67)90008-1, 1943.

Giordano, M., Beardall, J., and Raven, J. A.: CO_2 concentrating mechanisms in algae: mechanisms, environmental modulation and evolution, Annu. Rev. Plant Biol., 66:99–131, https://doi.org/10.1146/annurev.arplant.56.032604.144052, 2005.

Grice, A. M., Loneragan, N. R., and Dennison, W. C.: Light intensity and the interactions between physiology, morphology and stable isotope ratios in five species of seagrass. J. Exp. Mar. Biol. Ecol, 195(1), 91-110, https://doi.org/10.1016/0022-0981(95)00096-8, 1996.

Gowik, U., and Westhoff, P.: The path from C3 to C4 photosynthesis, Plant Physiol., 155(1), 56–63, https://doi.org/10.1104/pp.110.165308, 2012.

Harris, D., Horwáth, W. R., & Van Kessel, C.: Acid fumigation of soils to remove carbonates prior to total organic carbon or carbon-13 isotopic analysis, Soil Sci. Soc. Am. J., 65(6), 1853-1856, https://doi.org/10.2136/sssaj2001.1853, 2001.

Hepburn, C. D., Pritchard, D. W., Cornwall, C. E., McLeod, R. J., Beardall, J., Raven, J. A., and Hurd, C. L.: Diversity of carbon use strategies in a kelp forest community: implications for a high CO_2 ocean, Glob. Change Biol., 17, 2488–2497. https://doi.org/10.1111/j.1365-2486.2011.02411.x., 2011.

Hinger, E. N., Santos, G. M., Druffel, E. R. M., and Griffin, S.: Carbon isotope measurements of surface seawater from a time-series site off Southern California, Radiocarbon 52(1):69–89, 2010.

Hiraoka, M., Kinoshita, Y., Higa, M., Tsubaki, S., Monotilla, A. P., Onda, A., and Dan, A.: Fourfold daily growth rate in multicellular marine alga *Ulva meridionalis*, Scientific reports, 10(1), 1-7, 2020.

Hofmann, L., and Heesch, S.: Latitudinal trends in stable isotope signatures and carbon-concentrating mechanisms of northeast Atlantic rhodoliths, Biogeosciences, 15, 6139–6149, https://doi.org/10.5194/bg-15-6139-2018, 2018.

Hopkinson, B. M., Dupont, C. L., Allen, A. E., and Morel, F. M. M.: Efficiency of the CO_2-concentrating mechanism of diatoms, Proc. Natl. Acad. Sci. U.S.A., 108, 3830–3837, https://doi.org/10.1073/pnas.1018062108, 2011.

Hopkinson, B. M., Young, J. N., Tansik, A. L., and Binder, B. J.: The minimal CO_2 concentrating mechanism of *Prochlorococcus* MED4 is effective and efficient, *Plant Physiol.*, 166, 2205–2217, https://doi.org/10.1104/pp.114.247049, 2014.

Hu, X., Burdige, D. J., and Zimmerman, R. C.: $\delta^{13}C$ is a signature of light availability and photosynthesis in seagrass, Limnol. Oceanogr., 57(2), 441–448, https://doi.org/10.4319/lo.2012.57.2.0441, 2012.

Hurd, C. L.: Water motion, marine macroalgal physiology and production, J. Phycol., 36, 453–472, https://doi.org/10.1046/j.1529-8817.2000.99139.x, 2000.Iluz, D., Fermani, S., Ramot, M., Reggi, M., Caroselli, E., Prada, F., Dubinsky, Z., Goffredo, S. and Falin, G.: Calcifying response and recovery potential of the brown alga *Padina pavonica* under ocean acidification, ACS Earth Space Chem., 1(6), 316–323, https://doi.org/10.1021/acsearthspacechem.7b00051, 2017.

Iñiguez, C., Galmés, J., and Gordillo, F. J.: Rubisco carboxylation kinetics and inorganic carbon utilization in polar versus cold-temperate seaweeds, J. Exp. Bot., 70(4), 1283–1297. https://doi.org/10.1093/jxb/ery443, 2019.

Jensen, E. L., Maberly, S. C., and Gontero, B.: Insights on the functions and ecophysiological relevance of the diverse carbonic anhydrases in microalgae, Int. J. Mol. Sci., 21(8), 2922, https://doi.org/10.3390/ijms21082922, 2020.

Johansson, G., and Snoeijs, P.: Macroalgal photosynthetic responses to light in relation to thallus morphology and depth zonation, Mar. Ecol. Prog. Ser., 244, 63-72, https://doi:10.3354/meps244063, 2002.

Kevekordes, K., Holland, D., Häubner, N., Jenkins, S., Koss, R., Roberts, S., Raven, J.A., Scrimgeour, C.M., Shelly, K., Stojkovic, S. and Beardall, J.: Inorganic carbon acquisition by eight species of Caulerpa (Caulerpaceae, Chlorophyta), Phycologia, 45(4), 442-449, DOI:10.2216/05-55.1, 2006.

Kim, M. S., Lee, S. M., Kim, H. J., Lee, S. Y., Yoon, S. H., and Shin, K. H.: Carbon stable isotope ratios of new leaves of *Zostera marina* in the mid-latitude region: implications of seasonal variation in productivity, J. Exp. Mar Biol. Ecol*.,* 461, 286–296, https://doi.org/10.1016/j.jembe.2014.08.015, 2014.

Klenell, M., Snoeijs, P., and Pedersen, M.: Active carbon uptake in *Laminaria digitata* and *L. saccharina* (Phaeophyta) is driven by a proton pump in the plasma membrane, *Hydrobiologia,* 514, 41–53, https://doi.org/10.1023/B:hydr.0000018205.80186.3e, 2004.

Kroopnick, P. M.: The distribution of ^{13}C of ΣCO_2 in the world oceans. Deep Sea Res. Part I Oceanogr. Res. Pap, 32(1), 57-84, https://doi.org/10.1016/0198-0149(85)90017-2, 1985.

Kübler, J. E., and Davison, I. R.: High-temperature tolerance of photosynthesis in the red alga *Chondrus crispus,* Mar. Biol., 117(2), 327–335. https://doi.org/10.1007/BF00345678, 1993.

Kübler, J. E., and Raven, J. A.: The interaction between inorganic carbon acquisition and light supply in *Palmaria palmata* (Rhodophyta), J. Phycol., 31(3), 369-375, https://doi.org/10.1111/j.0022-3646.1995.00369.x,1995.

Kübler, J. E., and Raven, J. A.: Inorganic carbon acquisition by red seaweeds grown under dynamic light regimes, Hydrobiologia, 326(1), 401-406, 1996.

Kübler, J. E., and Dudgeon, S. R.: Predicting effects of ocean acidification and warming on algae lacking carbon concentrating mechanisms, *PLoS One,* 10 (7), https://doi.org/10.1371/journal.pone.0132806, 2015.

Lapointe, B. E., and Duke, C. S.: Biochemical strategies for growth of *Gracilaria tikvahiae* (Rhodophyta) in relation to light intensity and nitrogen availability, J. Phycol., 20(4), 488–495. https://doi.org/10.1111/j.0022-3646.1984.00488.x, 1984.

Littler, M. M., and Littler, D. S.: The evolution of thallus form and survival strategies in benthic marine macroalgae: field and laboratory tests of a functional form model, Am Nat., 116, 25–44, 1980.

Littler, M. M., and Arnold, K. E.: Primary productivity of marine macroalgal functional-form groups from south-western North America, J. Phycol., 18, 307–311, https://doi.org/10.1111/j.1529-8817.1982.tb03188.x, 1982.

Lobban, C. S., Harrison, P. J., and Harrison, P. J.: Seaweed ecology and physiology. Cambridge University Press, 1994.Lovelock, C. E., Reef, R., Raven, J. A., and Pandolfi, J. M.: Regional variation in δ^{13}C of coral reef macroalgae, Limnol. Oceanogr., https://doi.org/10.1002/lno.11453, 2020.

Lluch-Cota, S. E., Aragon-Noriega, E. A., Arreguin-Sanchez, F., Aurioles-Gamboa, D., Bautista-Romero, J. J., Brusca, R. C., Cervantes-Duarte, R., Cortes-Altamirano, R., Del-MonteLuna, P., Esquivel-Herrera, A., Fernández, G., Hendrickx, M. E., Hernandez-Vazquez, S., Herrera-Cervantes, H., Kahru, M., Lavin, M., Lluch-Belda, D., Lluch-Cota, D. B., Lopez-Martinez, J., Marinone, S. G., Nevarez-Martinez, M. O., Ortega-Garcia, S., Palacios-Castro, E., Pares-Sierra, A., Ponce-Diaz, G., RamirezRodriguez, M., Salinas-Zavala, C. A., Schwartzlose, R. A., and Sierra-Beltran, A. P.: The Gulf of California: Review of ecosystem status and sustainability challenges, Prog. Oceanogr., 73, 1–26, 2007.

Maberly, S. C., Raven, J. A. and Johnston, A. M.: Discrimination between ^{12}C and ^{13}C by marine plants, *Oecologia,* 91,481–492, https://doi.org/10.1007/BF00650320, 1992.

Mackey, A. P., Hyndes, G. A., Carvalho, M. C., and Eyre, B. D.: Physical and biogeochemical correlates of spatio-temporal variation in the δ^{13}C of marine macroalgae, Estuar. Coast. Shelf Sci., 157, 7-18, https://doi.org/10.1016/j.ecss.2014.12.040, 2015.

Madsen, T. V., and Maberly, S. C.: High internal resistance to CO_2 uptake by submerged macrophytes that use HCO_3^-: measurements in air, nitrogen and helium, Photosynth. Res., 77(2-3), 183–190, https://doi.org/10.1023/A:1025813515956, 2003.

Marinone, S. G., and Lavín, M. F.: Residual flow and mixing in the large islands' region of the central Gulf of California: Nonlinear processes in geophysical fluid dynamics, Springer, Dordrechm, http://doi-org-443.webvpn.fjmu.edu.cn/10.1007/978-94-010-0074-1_13, 2003.

Marinone, S. G.: A note on "Why does the Ballenas Channel have the coldest SST in the Gulf of California?". *Geophysical research letters*, 34(2). https://doi.org/10.1029/2006GL028589, 2007.

Marconi, M., Giordano, M., and Raven, J. A.: Impact of taxonomy, geography and depth on the δ^{13}C and δ^{15}N variation in a large collection of macroalgae, J. Phycol*.,* 47, 1023–1035, https://doi.org/10.1111/j.1529-8817.2011.01045.x, 2011.

Martínez-Díaz-de-León, A.: Upper-ocean circulation patterns in the Northern Gulf of California, expressed in Ers-2 synthetic aperture radar imagery, Cienc. Mar., 27(2), 209–221, https://doi.org/10.7773/cm.v27i2.465, 2001.

Martínez-Díaz-de-León, A., Pacheco-Ruíz, I., Delgadillo-Hinojosa, F., Zertuche-González, J. A., Chee-Barragán, A., Blanco-Betancourt, R., Guzmán-Calderón, J. M., and Gálvez-Telles, A.: Spatial and temporal variability of the sea surface temperature in the Ballenas-Salsipuedes Channel (central Gulf of California), J. Geophys. Res. Oceans*,* 111(C2), https://doi.org/10.1029/2005JC002940, 2006.

Masojidek, J., Kopecká, J., Koblížek, M., and Torzillo, G.: The xanthophyll cycle in green algae

(Chlorophyta): its role in the photosynthetic apparatus, Plant Biol., 6(3), 342–349, https://doi.org/10.1055/s-2004-820884, 2004.

McConnaughey, T. A., Burdett, J., Whelan, J. F., and Paull, C. K.: Carbon isotopes in biological carbonates: respiration and photosynthesis, Geochim. Cosmochim Ac., 61(3), 611–622, https://doi.org/10.1016/S0016-7037(96)00361-4, 1997.

Mercado, J. M., De los Santos, C. B., Pérez-Lloréns, J. L., and Vergara, J. J.: Carbon isotopic fractionation in macroalgae from Cadiz Bay (Southern Spain): comparison with other bio-geographic regions, Estuar, Coast. Shelf Sci., 85, 449–458, https://doi.org/10.1016/j.ecss.2009.09.005, 2009.

Mook, W. G., Bommerson, J. C., and Staverman, W. H.: Carbon isotope fractionation between dissolved bicarbonate and gaseous carbon dioxide, Earth Planet. Sci. Lett., 22(2), 169-176, https://doi.org/10.1016/0012-821X(74)90078-8, 1974.

Murru, M., and Sandgren, C.D.: Habitat matters for inorganic carbon acquisition in 38 species of red macroalgae (Rhodophyta) from Puget Sound, Washington, USA. J. Phycol., 40, 837–845. https://doi.org/10.1111/j.1529-8817.2004.03182.x, 2004.

Narvarte, B. C. V., Nelson, W. A., and Roleda, M. Y.: Inorganic carbon utilization of tropical calcifying macroalgae and the impacts of intensive mariculture-derived coastal acidification on the physiological performance of the rhodolith Sporolithon sp., Environ. Pollut., 266, 115344, https://doi.org/10.1016/j.envpol.2020.115344 , 2020.

Nielsen, S. L., and Jensen, K. S.: Allometric settling of maximal photosynthetic growth rate to surface/volume ratio, *Limnol. Oceanogra.*, 35(1), 177–180, https://doi.org/10.4319/lo.1990.35.1.0177, 1990.

Norris, J. N.: The marine algae of the northern Gulf of California, Ph. D. dissertation, University of California, Santa Barbara, 575 pp., 1975.

Norris, J. N.: Studies on *Gracilaria Grev*.(Gracilariaceae, Rhodophyta) from the Gulf of California, Mexico. Taxonomy of Economic Seaweeds, California Sea Grant College Program, California, I, 123-135, 1985.

Norris, J. N.: Marine algae of the northern Gulf of California: Chlorophyta and Phaoephyceae, Smithsonian contr. Bot., no. 94, https://doi.org/10.5479/si.19382812.96, 2010.

Ochoa-Izaguirre, M. J., Aguilar-Rosas, R., and Aguilar-Rosas, L. E.: Catálogo de Macroalgas de las lagunas costeras de Sinaloa, Serie Lagunas Costeras, Edited by Páez-Osuna, F., UNAM, ICMyL, México, pp 117, 2007.

Ochoa-Izaguirre, M. J., and Soto-Jiménez, M. F.: Variability in nitrogen stable isotope ratios of macroalgae: consequences for the identification of nitrogen sources, J. Phycol., 51, 46–65, https://doi.org/10.1111/jpy.12250, 2015.

Páez-Osuna, F., Piñón-Gimate, A., Ochoa-Izaguirre, M. J., Ruiz-Fernández, A. C., Ramírez-Reséndiz, G., and Alonso-Rodríguez, R.: Dominance patterns in macroalgal and phytoplankton biomass under different nutrient loads in subtropical coastal lagoons of the SE Gulf of California, Mar. Pollut. Bull., 77(1-2), 274-281, https://doi.org/10.1016/j.marpolbul.2013.09.048, 2013.

Páez-Osuna, F., Álvarez-Borrego, S., Ruiz-Fernández, A. C., García-Hernández, J., Jara-Marini, E., Bergés-Tiznado, M. E., Piñón-Gimate, A., Alonso-Rodríguez, R., Soto-Jiménez, M. F., Frías-Espericueta, M. G., Ruelas-Inzunza, J. R., Green-Ruíz, C. R., Osuna-Martínez, C. C., and Sánchez-Cabeza, J. A.: Environmental status of the Gulf of California: a pollution review, *Earth-Sci. Rev.*, 166, 181–205, https://doi.org/10.1016/j.earscirev.2016.09.015, 2017.

Pedroche, F. F., and Sentíes, A.: Ficología marina mexicana: Diversidad y Problemática actual, *Hidrobiológica*, 13(1), 23–32, 2003.

Rautenberger, R., Fernández, P. A., Strittmatter, M., Heesch, S., Cornwall, C. E., Hurd, C. L., and Roleda, M. Y.: Saturating light and not increased carbon dioxide under ocean acidification drive photosynthesis and growth in *Ulva rigida* (Chlorophyta), Ecol. Evol., 5(4), 874–888, https://doi.org/10.1002/ece3.1382, 2015.

Raven, J., Beardall, J., and Griffiths, H.: Inorganic C-sources for Lemanea, Cladophora, and Ranunculus in a fast-flowing stream: measurements of gas exchange and of carbon isotope ratio and their ecological implications, Oecologia, 53: 68–78, doi: 10.1007/BF00377138.,1982.

Raven, J. A., Johnston, A. M., Kübler, J. E., Korb, R. E., McInroy, S. G., Handley, L. L., Scrimgeour, C. M., Walker, D. I., Beardall, J., Clayton, M. N., Vanderklift, M., Fredriksen, S., and Dunton, K. H.: Seaweeds in cold seas: evolution and carbon acquisition, Ann. Bot*.,* 90, 525–536. https://doi.org/10.1093/aob/mcf171, 2002a.

Raven, J. A., Johnshton, A. M., Kübler, J. E., Korb, R. E., Mclnroy, S. G., Handley, L. L., Scrimgeour, C. M., Walker, D. I., Beardall, J., Vanderklift, M., Fredriksen, S., and Dunton, K. H.: Mechanistic interpretation of carbon isotope discrimination by marine macroalgae and seagrasses, Funct. Plant Biol*.,* 29:355–378, https://doi.org/10.1071/PP01201, 2002b.

Raven, J. A., Ball, L. A., Beardall, J., Giordano, M., and Maberly, S. C.: Algae lacking carbon-concentrating mechanisms, Can. J. Bot., 83(7), 879–890, https://doi.org/10.1139/b05-074, 2005.

Raven, J. A., and Beardall, J.: The ins and outs of CO_2, J. Exp. Bot., *67*(1), 1–13, https://doi.org/10.1093/jxb/erv451, 2016.

Roberts, K., Granum, E., Leegood, R. C., and Raven, J. A.: C3 and C4 pathways of photosynthetic carbon assimilation in marine diatoms are under genetic, not environmental control, Plant Physiol., 145(1), 230–235, https://doi.org/10.1104/pp.107.102616, 2007.

Robles-Tamayo, C. M., Valdez-Holguín, J. E., García-Morales, R., Figueroa-Preciado, G., Herrera-Cervantes, H., López-Martínez, J., and Enríquez-Ocaña, L. F.: Sea surface temperature (SST) variability of the eastern coastal zone of the gulf of California. Remote Sensing, 10(9), 1434, https://doi.org/10.3390/rs10091434, 2018.
Roden, G. I.: Oceanographic and meteorological aspects of the Gulf of California, 1958.

Roden, G. I., and Groves, G. W.: Recent oceanographic investigations in the Gulf of California, J. Mar. Res., 18(1), 10–35, 1959.

Roden, G. I., and Emilsson, L.: Physical oceanography of the Gulf of California. Simposium Golfo de California, Universidad Nacional Autónoma de México, Mazatlán, Sinaloa, México, 1979.

Rusnak, G. A., Fisher, R. L., and Shepard, F. P.: Bathymetry and faults of Gulf of California. In: van Andel, Tj. H. and G.G. Shor, Jr. (editors), Marine Geology of the Gulf of California: A symposium, *AAPG Memoir*, 3, 59–75, https://doi.org/10.1306/M3359C3, 1964.

Sand-Jensen, K., and Gordon, D.: Differential ability of marine and freshwater macrophytes to utilize HCO_3^- and CO_2, Mar. Biol*.,* 80, 247–253, https://doi.org/10.1111/j.1469-8137.1981.tb03198.x, 1984.

Sanford, L. P., and Crawford, S. M.: Mass transfer versus kinetic control of uptake across solid-water boundaries, Limnol. Oceanogr., 45, 1180−1186, https://doi.org/10.4319/lo.2000.45.5.1180, 2000.

Santamaría-del-Angel, E., Alvarez-Borrego, S., and Müller-Karger, F. E.: Gulf of California biogeographic regions based on coastal zone color scanner imagery, J. Geophys. Res., 99, 7411–7421, https://doi.org/10.1029/93JC02154, 1994.

Santos, G. M., Ferguson, J., Acaylar, K., Johnson, K. R., Griffin, S., and Druffel, E.: Δ^{14}C and δ^{13}C of seawater DIC as tracers of coastal upwelling: A 5-year time series from Southern California, Radiocarbon, 53(4), 669-677, https://doi.org/10.1017/S0033822200039126, 2011.

Setchell, W., and Gardner, N.: The marine algae of the Pacific Coast of North America. Part II Chlorophyceae, Univ. Calif. Publ. Bot., 8, 139–374, https://doi.org/10.5962/bhl.title.5719, 1920.

Setchell, W., and Gardner, N.: The marine algae: Expedition of the California Academy of Sciences to the Gulf of California in 1921, Proc. Calif. Acad. Sci*., 4th series,* 12(29), 695–949, 1924.

Sharkey, T. D., and Berry, J. A.: Carbon isotope fractionation of algae as influenced by an inducible CO_2 concentrating mechanism. Inorganic carbon uptake by aquatic photosynthetic organisms, 1985.

Stepien, C. C.: Impacts of geography, taxonomy and functional group on inorganic carbon use patterns in marine macrophytes, J. Ecol., 103(6), 1372–1383, https://doi.org/10.1111/1365-2745.12451, 2015.

Teichberg, M., Fox, S. E., Olsen, Y. S., Valiela, I., Martinetto, P., Iribarne, O., Muto, E. Y., Petti, M. A., Cobrisier, T. N., Soto-Jiménez, M., Páez-Osuna, F., Castro, P., Freitas, H., Zitelli, A., Cardinaletti, M. and Tagliapietra, D.: Eutrophication and macroalgal blooms in temperate and tropical coastal waters: nutrient enrichment experiments with Ulva spp., Global Change Biology, 16(9), 2624-2637, https://doi.org/10.1111/j.1365-2486.2009.02108.x, 2010.

Valiela, I., Liu, D., Lloret, J., Chenoweth, K., and Hanacek, D.: Stable isotopic evidence of nitrogen sources and C4 metabolism driving the world’s largest macroalgal green tides in the Yellow Sea, Sci. Rep., 8(1), 1–12, https://doi.org/10.1038/s41598-018-35309-3, 2018.

Vásquez-Elizondo, R. M., and Enríquez, S.: Light absorption in coralline algae (Rhodophyta): a morphological and functional approach to understanding species distribution in a coral reef lagoon, Front. Mar. Sci., 4, 297, https://doi.org/10.3389/fmars.2017.00297, 2017.

Vásquez-Elizondo, R. M., Legaria-Moreno, Pérez-Castro, M.A., Krämer, W. E., Scheufen, T., Iglesias-Prieto, R., and Enríquez, S.: Absorptance determinations on multicellular tissues, Photosynth, Res., 132, 311–324, https://doi.org/10.1007/s11120-017-0395-6, 2017.

Velasco-Fuentes, O. V., and Marinone, S. G.: A numerical study of the Lagrangian circulation in the Gulf of California, J. Mar. Syst., 22(1), 1–12. https://doi.org/10.1016/S0924-7963(98)00097-9, 1999.

Young, E. B., and Beardall, J.: Modulation of photosynthesis and inorganic carbon acquisition in a marine microalga by nitrogen, iron, and light availability, Can. J. Bot., 83(7), 917–928, https://doi.org/10.1139/b05-081, 2005.

Young, J. N., Heureux, A. M., Sharwood, R. E., Rickaby, R. E., Morel, F. M., and Whitney, S. M.: Large variation in the Rubisco kinetics of diatoms reveals diversity among their carbon-concentrating mechanisms, J. Exp. Bot., 67(11), 3445–3456, https://doi.org/10.1093/jxb/erw163, 2016.

Xu, J., Fan, X., Zhang, X., Xu, D., Mou, S., Cao, S., Zheng, Z., Miao, J., Ye, N.: Evidence of coexistence of C3 and C4 photosynthetic pathways in a green-tide-forming alga, *Ulva prolifera, PloS one*, 7(5), e37438, https://doi.org/10.1371/journal.pone.0037438, 2012.

Xu, J., Zhang, X., Ye, N., Zheng, Z., Mou, S., Dong, M., Xu, D. and Miao, J.: Activities of principal photosynthetic enzymes in green macroalga *Ulva linza*: functional implication of C4 pathway in CO_2 assimilation, Sci. China Life Sci., 56(6), 571–580, https://doi.org/10.1007/s11427-013-4489-x, 2013.

Wefer, G., and Berger, W. H.: Stable isotope composition of benthic calcareous algae from Bermuda, J. Sediment. Res., 51(2), 459–465, https://doi.org/10.1306/212F7CAC-2B24-11D7-8648000102C1865D, 1981.

Wilkinson T. E., Wiken, J., Bezaury-Creel, T., Hourigan, T., Agardy, H., Herrmann, L., Janishevski, C. Madden, L. Morgan and M. Padilla.: Marine Ecoregions of North America. CEC, Montreal, Canada, 2009.

Zabaleta, E., Martin, M. V., and Braun, H. P.: A basal carbon concentrating mechanism in plants?, Plant Sci., 187, 97–104, https://doi.org/10.1016/j.plantsci.2012.02.001, 2012.

Zeebe, R. E., and Wolf-Gladrow, D.: CO_2 in seawater: equilibrium, kinetics, isotopes (No. 65) Gulf Professional Publishing, 2001.

Zeitzschel, B.: Primary productivity in the Gulf of California, Mar. Biol., 3(3), 201–207, https://doi.org/10.1007/BF00360952, 1969.

Zou, D., Xia, J., and Yang, Y.: Photosynthetic use of exogenous inorganic carbon in the agarophyte *Gracilaria lemaneiformis* (Rhodophyta), Aquac*,* 237, 421-431, https://doi.org/10.1016/j.aquaculture.2004.04.020, 2004.

Figure captions

Fig. 1. Sites collection along the continental (C1-C3) and peninsula (P1-P3) Gulf of California coastlines (A), range of environmental factors supporting or limiting the life processes for the macroalgal communities within a habitat (B), and inserted Table with the features and environmental conditions in the diverse habitats in the GC bioregions that delimits the macroalgal community's zonation.

Fig. 2. Variability of $\delta^{13}C$ values for specimens of different macroalgae genera collected along GC coastlines classified by taxon: (A) Chlorophyta, (B) Ochrophyta and (C) Rhodophyta. Shaded background represents the cutoff limits for using CO_2 Only users and HCO_3^- only users, respectively, according to Raven et al., (2002).

Fig. 3. Variability of $\delta^{13}C$ values for the genus collected along coastline of the Gulf of California according to their taxon: (A) Chlorophyta, (B) Ochrophyta and (C) Rhodophyta. Genus with n=1 is not shown, and genus n=2 was not considered to the statistical comparison. Different letters indicate significant differences ($P<0.05$): a>b>c>d>e. Shaded background represent the cutoff limits for using CO2 Only users and HCO3- only users, respectively, according to Raven et al., (2002). For Chlorophyta: Bry= *Bryopsis*, Cau=*Caulerpa*, Cha= *Chaetomorpha*, Cla= *Cladophora*, Cod= *Codium*, Phy= *Phyllodictyon*, Str= *Struveopsis*, Ulv=*Ulva.* Phaeophyta: Col= *Colpomenia*, Dic= *Dictyota*, Ect= *Ectocarpus*, End= *Endarachne*, Hyd= *Hydroclathatrus*, Pad= *Padina*, Ros= *Rosenvingea*, Sar= *Sargassum*, Spa= *Spatoglossum*, Zon= *zonaria.* Rhodophyta: Aca: *Acantophora*, anf: *Anfeltiopsis*, Amp= *Amphiroa*, Cen= *Centroceras*, Cer^1= *Ceramium*, Cer^2 = *Ceratodictyon*, Cho^1= *Chondracanthus*, Cho^2= *Chondria*, Das= *Dasya*, Dig= *Digenia*, Euc= *Euchema*, Gel= *Gelidium*, Gig= *Gigartina*, Gra^1= *Gracilaria*, Gra^2= *Grateloupia*, Gra^3=

Gracilariopsis, Gym= *Gymnogongrus*, Hal= *Halymenia*, Hyp= *Hypnea*, Jan= Jania, Lau= Laurencia, Lom= *Lomentaria*, Neo= *Neosiphonia*, Pol= *Polysiphonia*, Pri= *Prionitis*, Rho^1= *Rhodoglossum*, Rho^2= *Rhodymenia*,Sch= *Schizymenia*, Spy= *Spyridia*, Tac= *Tacanoosca*. Purple boxplots represent calcifying species group.

Fig. 4. Variability of δ^{13}C values for morphofunctional groups by taxa along coastline of the Gulf of California.

Fig. 5 Proportion of species using different DIC sources according to their carbon uptake strategies: HCO_3^- only users (CO_2 concentrating mechanism active), Users of both sources (HCO_3^- & CO_2) and CO_2 only users (non-CO_2 concentrating mechanism active) in function of coast along GC.

Fig. 6. Variability of δ^{13}C values in macroalgae specimens for the most representative genera in function of habitat features (emersion level). Green circles represent genus of Chlorophyta, Brown circles represent genus of Ochrophyta; red circles represent genus Rhodophyta and purple circles represent genus with calcifying capacity.

Fig. 7. Variability of δ^{13}C values in macroalgae specimens for the most representative genus in function of temperature (a) and pH (b) ranges in samples collected along Gulf of California coastline.

Fig. 8. Proportion of species using different DIC sources according to their carbon assimilation strategies: HCO_3^- only users (CO_2 concentrating mechanism active), Users of both sources (HCO_3^- & CO_2) and CO_2 only users (non-CO_2 concentrating mechanism active) in function of : (A) pH ranges, (B) temperature ranges and (C) salinity ranges.

Fig. 9. Trends in the δ^{13}C-macroalgal in specimens collected along continental (C1-C3) and peninsula (P1-P3) Gulf of California coastline in function of latitudinal gradient.

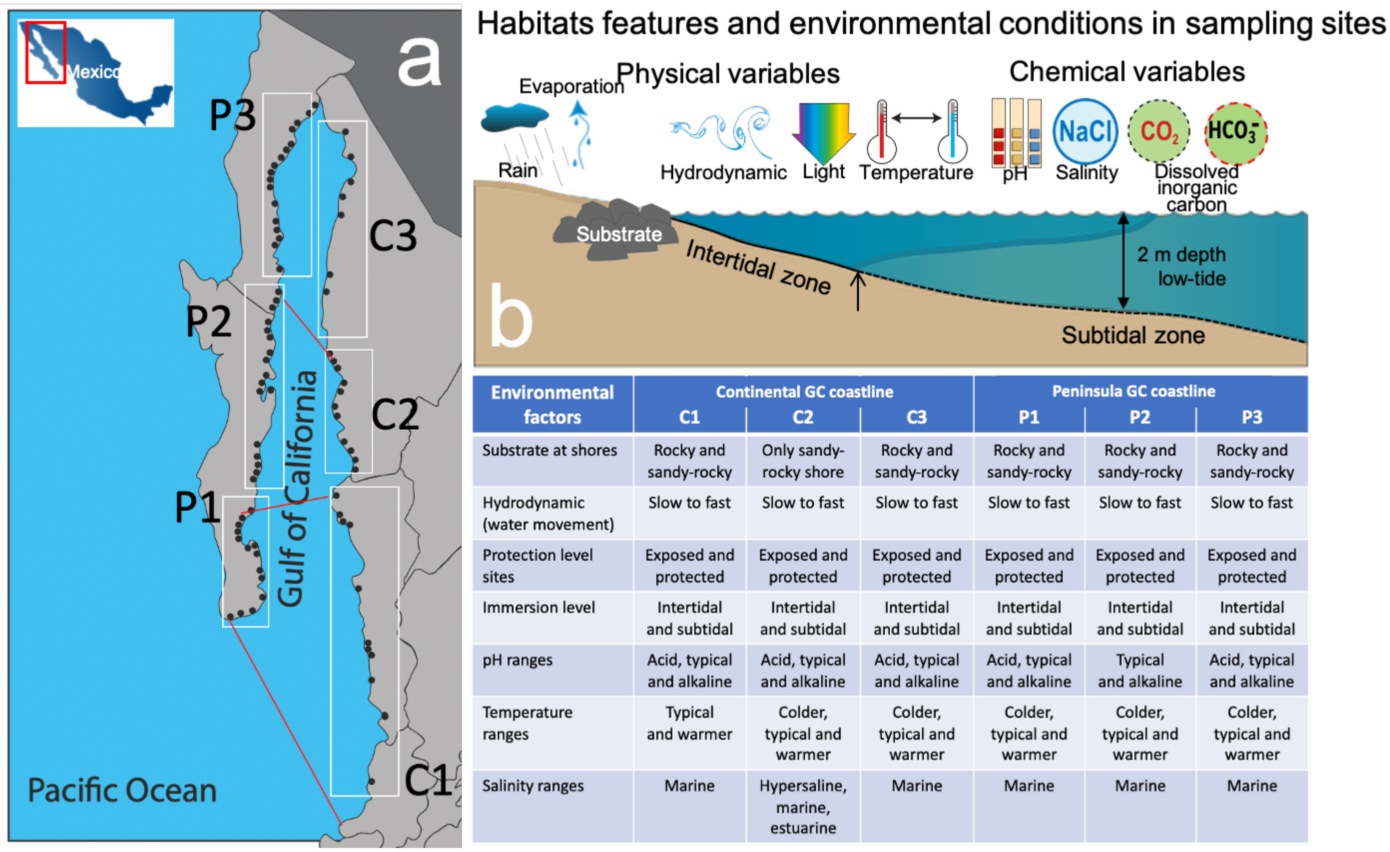

Environmental factors	Continental GC coastline			Peninsula GC coastline		
	C1	C2	C3	P1	P2	P3
Substrate at shores	Rocky and sandy-rocky	Only sandy-rocky shore	Rocky and sandy-rocky	Rocky and sandy-rocky	Rocky and sandy-rocky	Rocky and sandy-rocky
Hydrodynamic (water movement)	Slow to fast	Slow to fast	Slow to fast	Slow to fast	Slow to fast	Slow to fast
Protection level sites	Exposed and protected	Exposed and protected	Exposed and protected	Exposed and protected	Exposed and protected	Exposed and protected
Immersion level	Intertidal and subtidal	Intertidal and subtidal	Intertidal and subtidal	Intertidal and subtidal	Intertidal and subtidal	Intertidal and subtidal
pH ranges	Acid, typical and alkaline	Acid, typical and alkaline	Acid, typical and alkaline	Acid, typical and alkaline	Typical and alkaline	Acid, typical and alkaline
Temperature ranges	Typical and warmer	Colder, typical and warmer	Colder, typical and warmer	Colder, typical and warmer	Colder, typical and warmer	Colder, typical and warmer
Salinity ranges	Marine	Hypersaline, marine, estuarine	Marine	Marine	Marine	Marine

Fig. 1

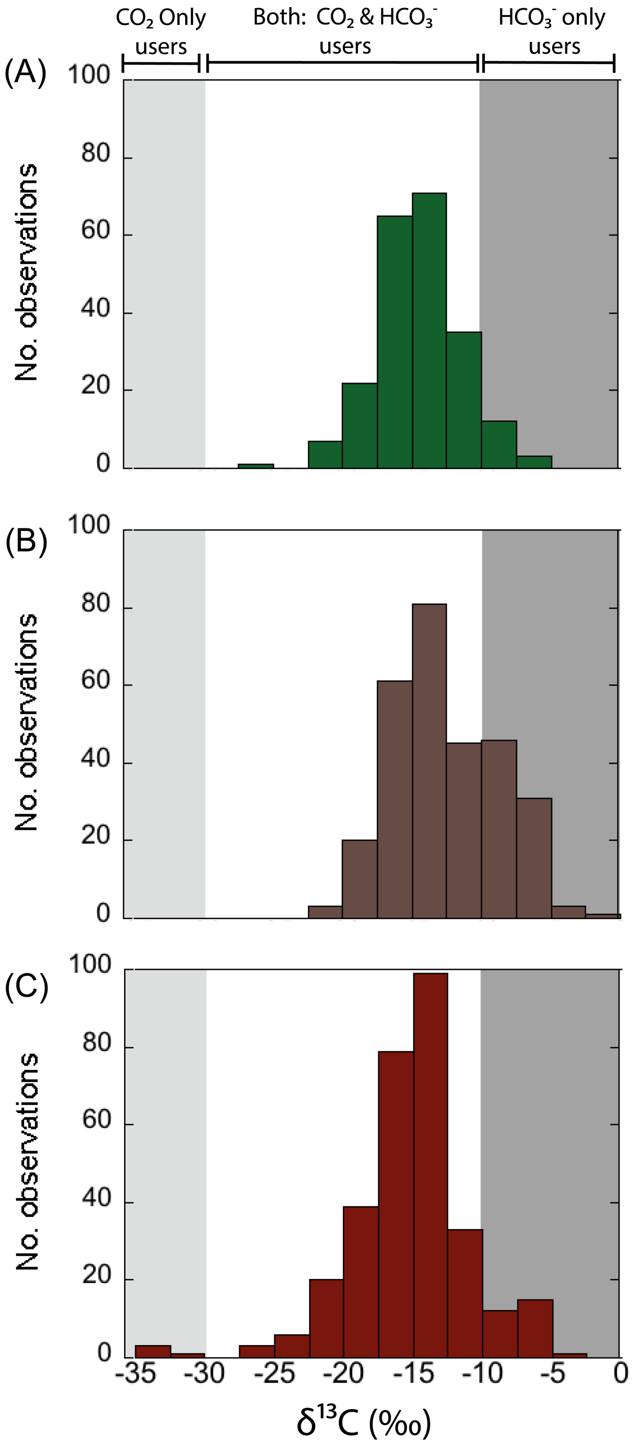
CO$_2$ Only users
Both: CO$_2$ & HCO$_3^-$ users
HCO$_3^-$ only users
(A)
(B)
(C)
No. observations
0
20
40
60
80
100
-35
-30
-25
-20
-15
-10
-5
0
δ^{13}C (‰)

Fig 2

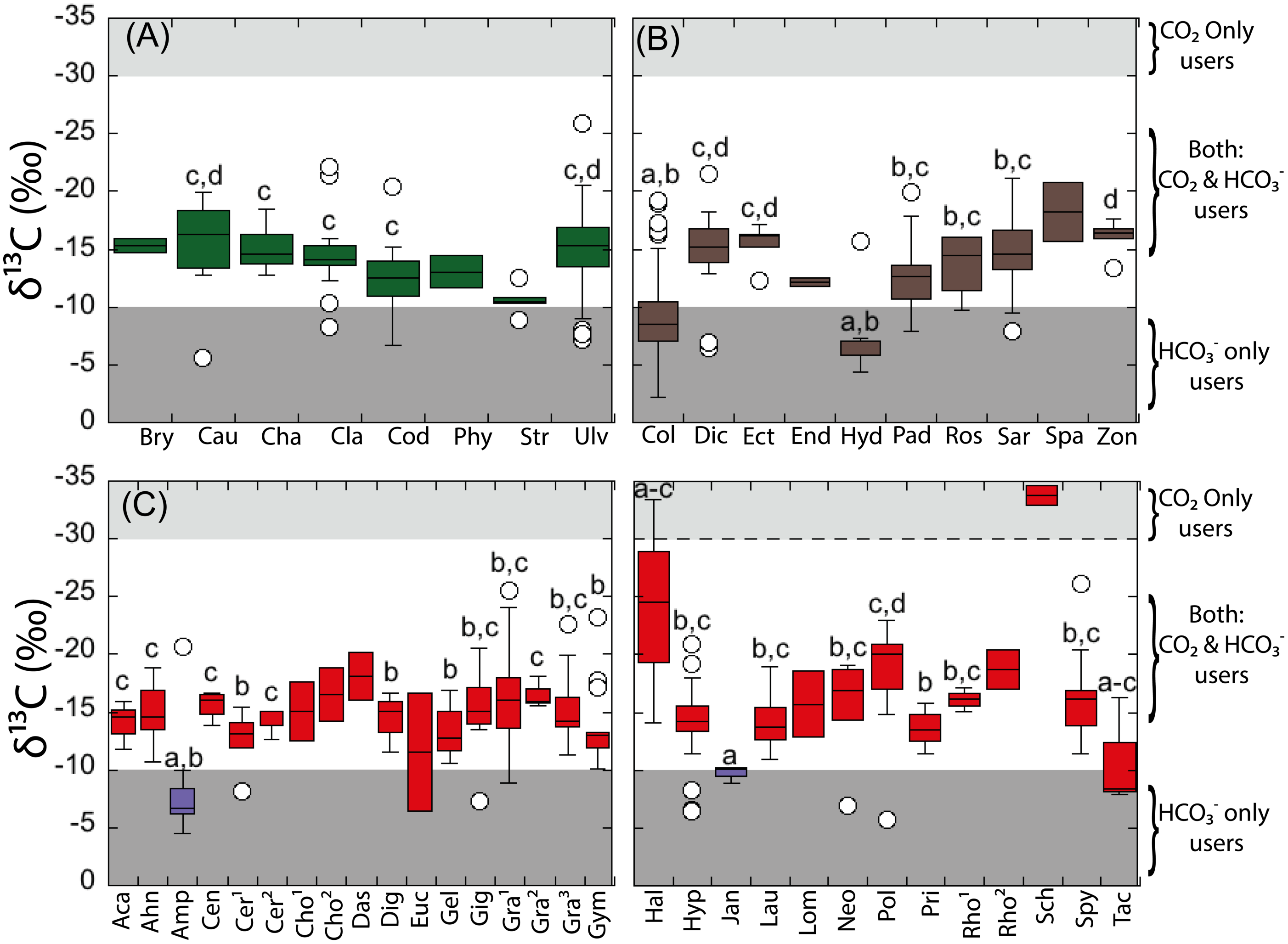
(A)
(B)
(C)
δ13C (‰)
-35
-30
-25
-20
-15
-10
-5
0
Bry
Cau
Cha
Cla
Cod
Phy
Str
Ulv
c,d
c
c
c
c,d
Col
Dic
Ect
End
Hyd
Pad
Ros
Sar
Spa
Zon
a,b
c,d
c,d
a,b
b,c
b,c
b,c
d
CO2 Only users
Both: CO2 & HCO3- users
HCO3- only users
Aca
Ahn
Amp
Cen
Cer1
Cer2
Cho1
Cho2
Das
Dig
Euc
Gel
Gig
Gra1
Gra2
Gra3
Gym
c
c
a,b
c
b
c
b
b
b,c
b,c
c
b,c
b
Hal
Hyp
Jan
Lau
Lom
Neo
Pol
Pri
Rho1
Rho2
Sch
Spy
Tac
a-c
b,c
a
b,c
b,c
c,d
b
b,c
b,c
a-c

Fig 3

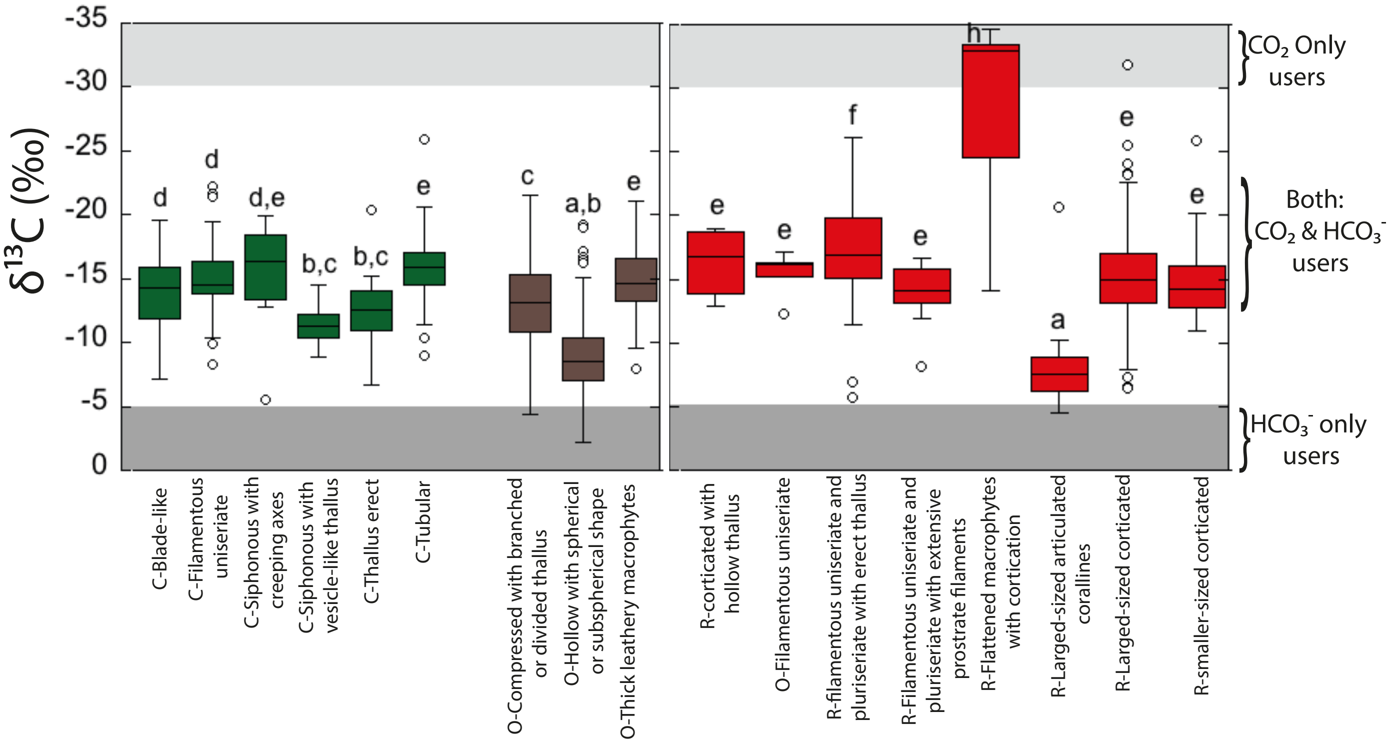
δ^{13}C (‰)
-35
-30
-25
-20
-15
-10
-5
0
d
d
d,e
b,c
b,c
e
c
a,b
e
e
e
f
e
h
a
e
e
CO$_2$ Only users
Both: CO$_2$ & HCO$_3^-$ users
HCO$_3^-$ only users
C-Blade-like
C-Filamentous uniseriate
C-Siphonous with creeping axes
C-Siphonous with vesicle-like thallus
C-Thallus erect
C-Tubular
O-Compressed with branched or divided thallus
O-Hollow with spherical or subspherical shape
O-Thick leathery macrophytes
R-corticated with hollow thallus
O-Filamentous uniseriate
R-filamentous uniseriate and pluriseriate with erect thallus
R-Filamentous uniseriate and pluriseriate with extensive prostrate filaments
R-Flattened macrophytes with cortication
R-Larged-sized articulated corallines
R-Larged-sized corticated
R-smaller-sized corticated

Fig 4

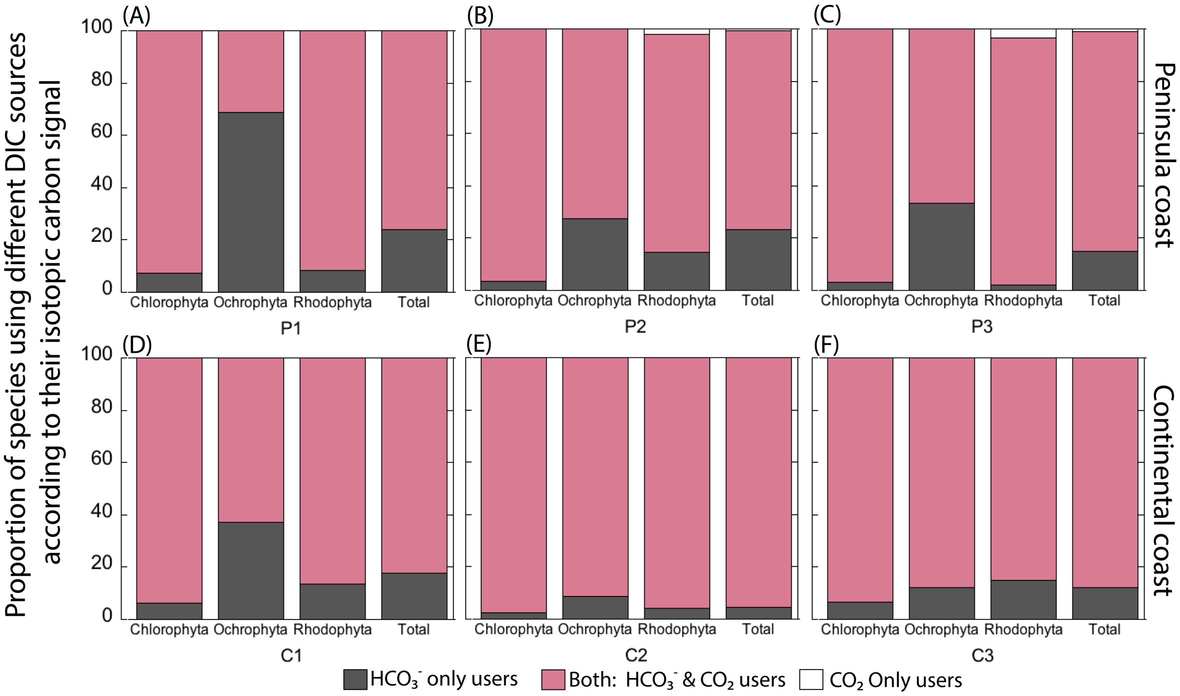
Proportion of species using different DIC sources according to their isotopic carbon signal
(A)
(B)
(C)
(D)
(E)
(F)
100
80
60
40
20
0
Chlorophyta
Ochrophyta
Rhodophyta
Total
P1
P2
P3
C1
C2
C3
Peninsula coast
Continental coast
HCO3- only users
Both: HCO3- & CO2 users
CO2 Only users

1286 **Fig 5**

1287

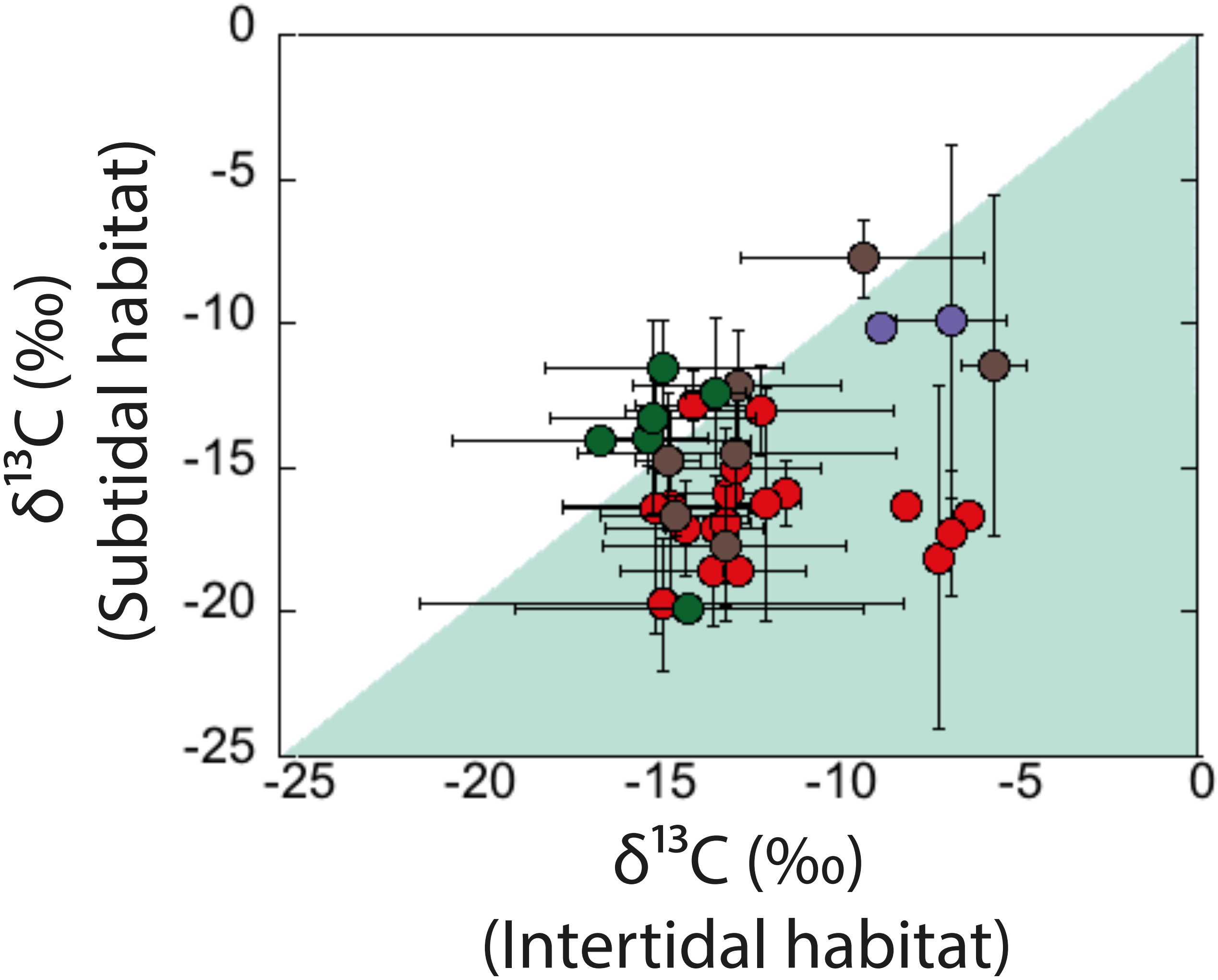

1288

1289 **Fig 6**

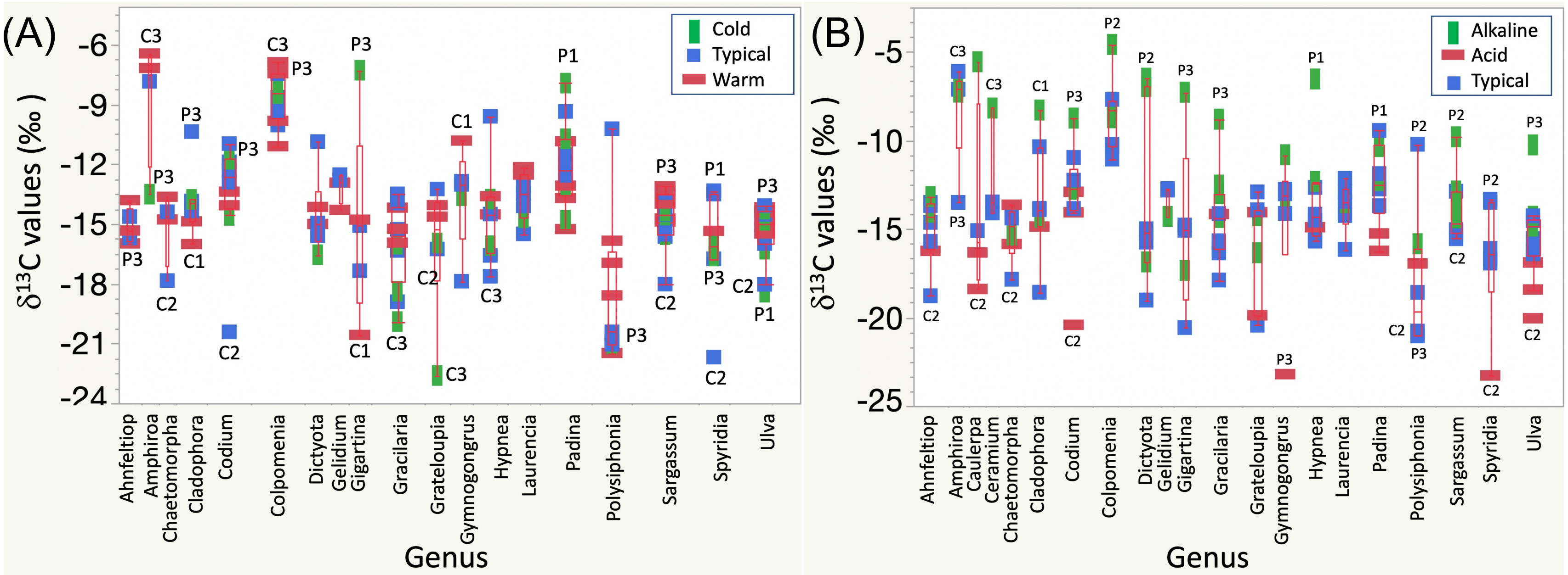
(A)
-6
-9
-12
-15
-18
-21
-24
δ13C values (‰)
Cold
Typical
Warm
C3
P3
P3
C2
P3
C1
P3
C2
C3
P3
P3
C1
C1
C2
C3
C3
C3
P1
P3
P3
C2
P1
P3
C2
P3
C2
P1
Ahnfeltiop
Amphiroa
Chaetomorpha
Cladophora
Codium
Colpomenia
Dictyota
Gelidium
Gigartina
Gracilaria
Grateloupia
Gymnogongrus
Hypnea
Laurencia
Padina
Polysiphonia
Sargassum
Spyridia
Ulva
Genus
(B)
-5
-10
-15
-20
-25
δ13C values (‰)
Alkaline
Acid
Typical
C3
P3
C2
C3
C2
C2
C1
P3
C2
P2
P2
P3
P3
P3
P1
P1
P2
C2
P3
P2
C2
P2
C2
P3
C2
Ahnfeltiop
Amphiroa
Caulerpa
Ceramium
Chaetomorpha
Cladophora
Codium
Colpomenia
Dictyota
Gelidium
Gigartina
Gracilaria
Grateloupia
Gymnogongrus
Hypnea
Laurencia
Padina
Polysiphonia
Sargassum
Spyridia
Ulva
Genus

Fig 7

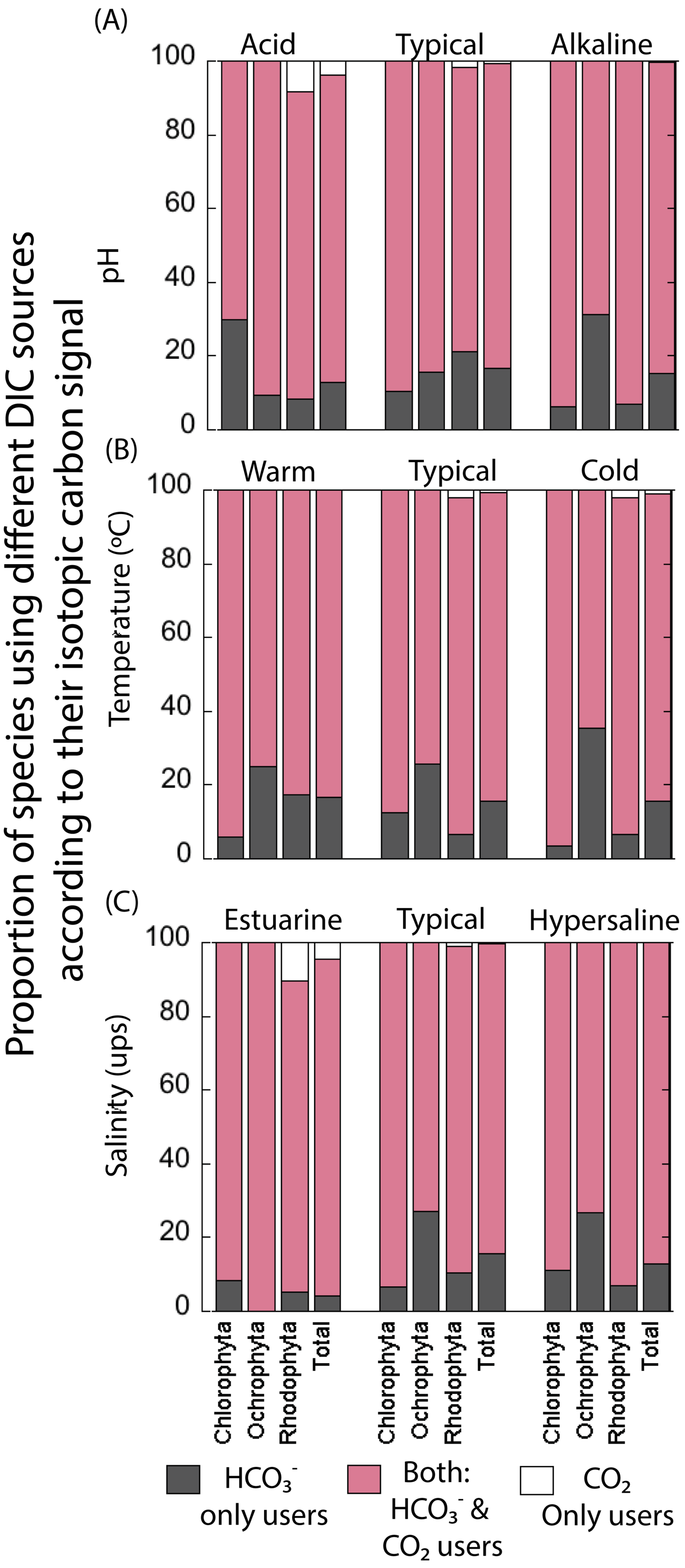

(A)
Acid
Typical
Alkaline
pH
100
80
60
40
20
0
(B)
Warm
Typical
Cold
Temperature (°C)
100
80
60
40
20
0
(C)
Estuarine
Typical
Hypersaline
Salinity (ups)
100
80
60
40
20
0
Proportion of species using different DIC sources according to their isotopic carbon signal
Chlorophyta
Ochrophyta
Rhodophyta
Total
Chlorophyta
Ochrophyta
Rhodophyta
Total
Chlorophyta
Ochrophyta
Rhodophyta
Total
HCO3- only users
Both: HCO3- & CO2 users
CO2 Only users

Fig 8

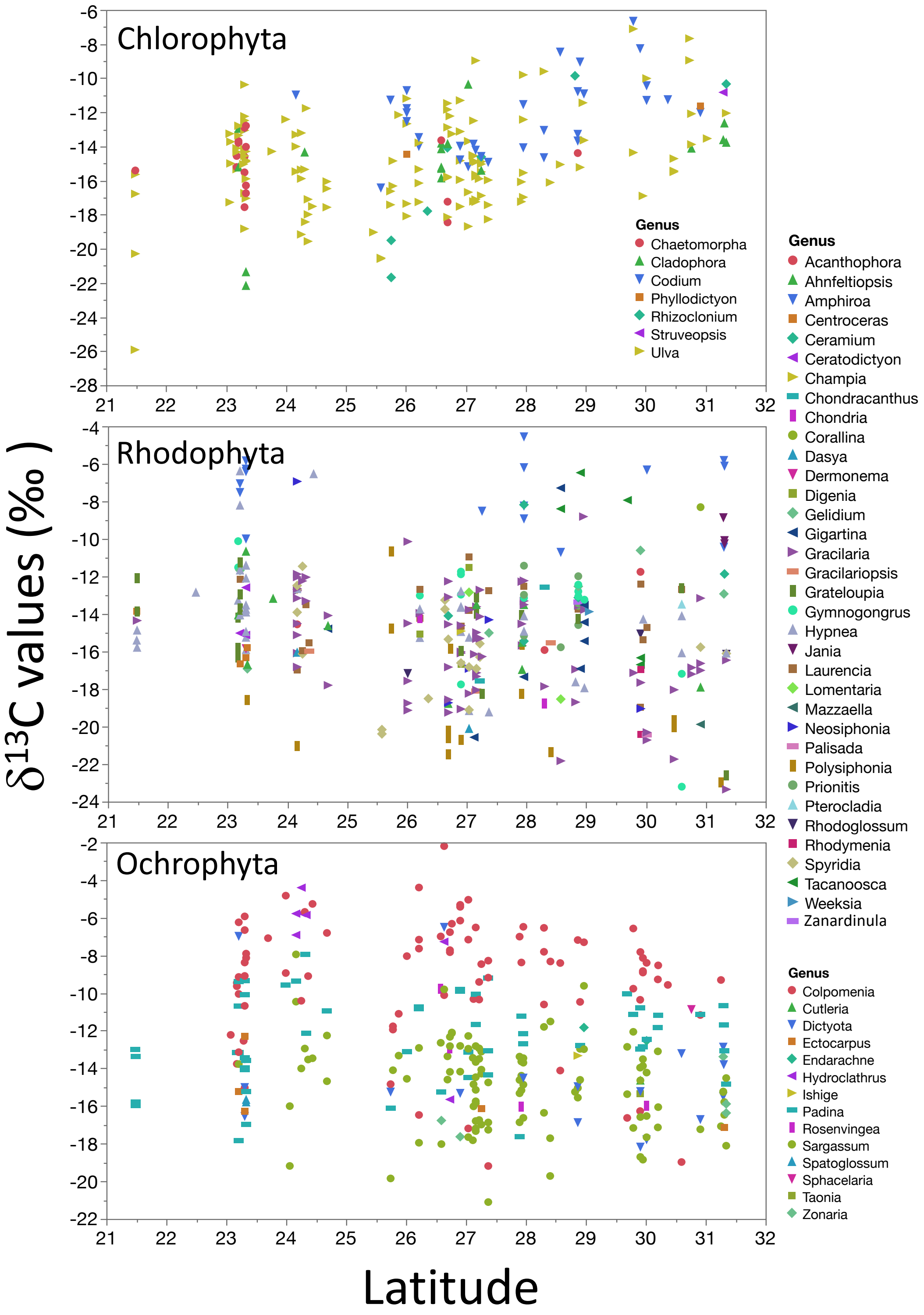
Chlorophyta
Genus
Chaetomorpha
Cladophora
Codium
Phyllodictyon
Rhizoclonium
Struveopsis
Ulva
-6
-8
-10
-12
-14
-16
-18
-20
-22
-24
-26
-28
Rhodophyta
-4
-6
-8
-10
-12
-14
-16
-18
-20
-22
-24
Ochrophyta
-2
-4
-6
-8
-10
-12
-14
-16
-18
-20
-22
21
22
23
24
25
26
27
28
29
30
31
32
δ13C values (‰)
Latitude
Genus
Acanthophora
Ahnfeltiopsis
Amphiroa
Centroceras
Ceramium
Ceratodictyon
Champia
Chondracanthus
Chondria
Corallina
Dasya
Dermonema
Digenia
Gelidium
Gigartina
Gracilaria
Gracilariopsis
Grateloupia
Gymnogongrus
Hypnea
Jania
Laurencia
Lomentaria
Mazzaella
Neosiphonia
Palisada
Polysiphonia
Prionitis
Pterocladia
Rhodoglossum
Rhodymenia
Spyridia
Tacanoosca
Weeksia
Zanardinula
Genus
Colpomenia
Cutleria
Dictyota
Ectocarpus
Endarachne
Hydroclathrus
Ishige
Padina
Rosenvingea
Sargassum
Spatoglossum
Sphacelaria
Taonia
Zonaria

Fig. 9

1296

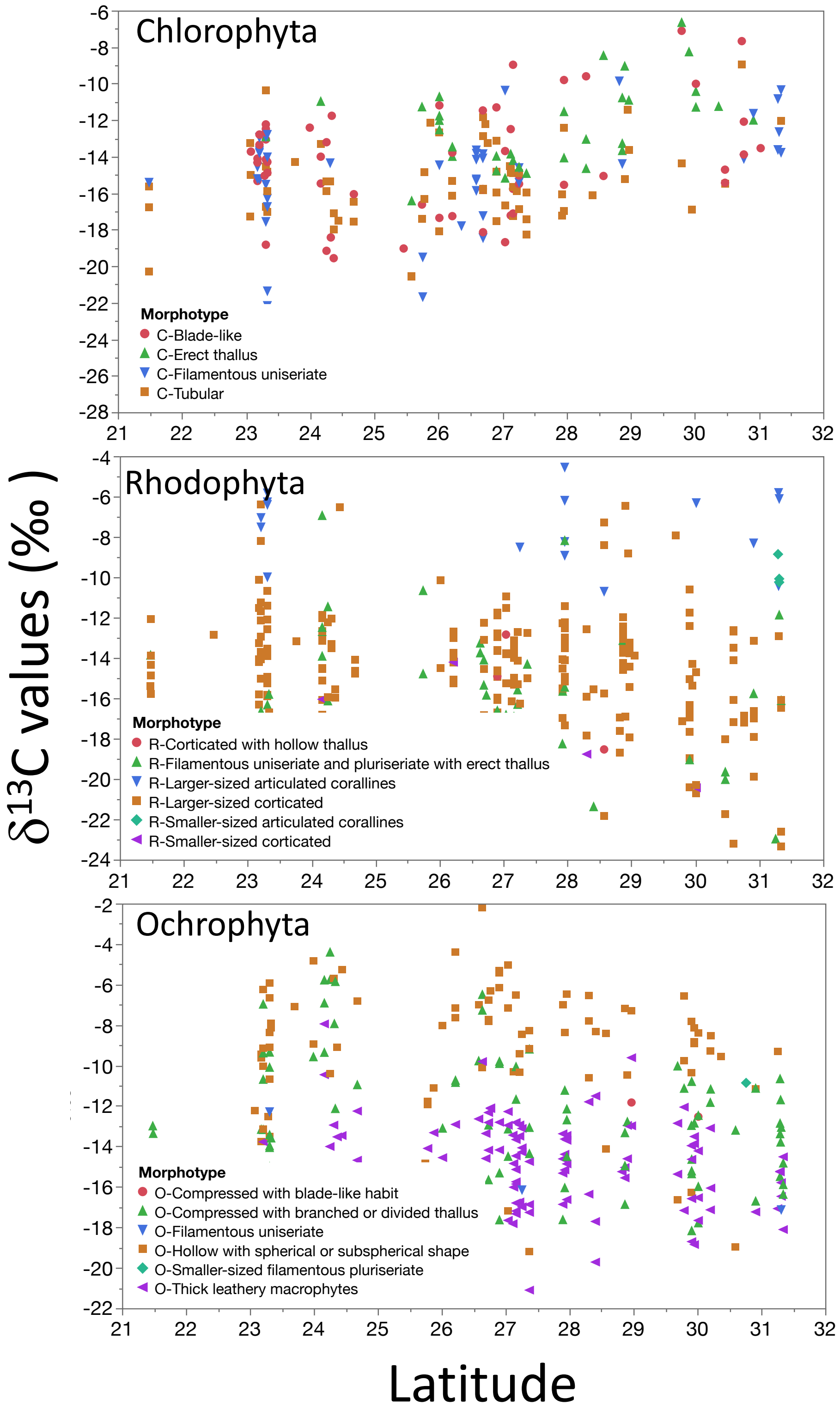

1297 **Fig. 10**

Table 1. Carbon isotopic composition (‰) in species of Phylum Chlorophyta collected along Gulf of California coastlines.

Species (n composite samples)	δ^{13}C±SD (Min to Max, ‰)
Chaetomorpha sp. (3)	-13.7±0.8 (-14.6 to -12.9)
C. antennina (10)	-14.6±1.1 (-16.3 to -12.8)
C. linum (5)	-16.8±1.6 (-18.4 to -14.6)
Codium sp. (5)	-11.6±3.0 (-14.1 to-6.7)
C. amplivesiculatum (8)	-14.4±2.7 (-20.4 to -11.3)
C. brandegeei (7)	-11.8±1.2 (-13.7 to -10.4)
C. fragile (4)	-13.0±2.7 (-14.8 to -9.0)
C. simulans (9)	-11.4±2.2 (-14.9 to -8.3)
Ulva sp. (12)	-14.0±3.9 (-19.2 to -7.1)
U. acanthophora (25)	-15.8±1.7 (-18.3 to -11.4)
U. clathrata (8)	-16.4± 2.0 (-20.5 to -14.5)
U. compressa (4)	-17.8±2.4 (-20.6 to -15.4)
U. flexuosa (13)	-16.0±3.7 (-25.9 to -10.4)
U. intestinalis (16)	-15.3±2.5 (-20.3 to -8.9)
U. lactuca (31)	-14.1±3.1 (-19.6 to -7.7)
U. linza (6)	-15.6±2.4 (-19.4 to -13.2)
U. lobata (5)	-13.2±1.9 (-15.3 to -11.1)
U. prolifera (3)	-14.2±1.8 (-15.5 to -12.2)

Table 2. Carbon isotopic composition (‰) in species of Phylum Ochrophyta collected along Gulf of California coastlines.

Species (n composite samples)	δ^{13}C±SD (Min to Max, ‰)
Colpomenia sp. (11)	-11.0±3.7 (-19.0 to -5.4)
C. ramosa (4)	-11.4±2.6 (-13.8 to-7.8)
C. sinuosa (7)	-10.2±3.0 (-16.3 to -7.2)
C. tuberculata (64)	-8.7±3.2 (-19.2 to -2.2)
Padina sp. (15)	-11.1±1.5 (-13.1 to-7.9)
P. crispata (3)	-11.3±1.7 (-12.5 to -10.1)
P. durvillei (36)	-13.2±2.6 (-20.0 to -9.2)
Sargassum sp. (34)	-14.3±2.4 (-18.7 to -8.0)
S. herporhizum (7)	-13.7±1.6 (-16.6 to -11.5)
S. horridum (12)	-15.5±2.9 (-19.7 to-9.5)
S. johnstonii (10)	-15.4±2.0 (-17.7 to -11.8)
S. lapazeanum (7)	-14.5±1.6 (-17.2 to -12.8)
S. sinicola (31)	-15.1±2.4 (-21.1 to -12.1)

Table 3. Carbon isotopic composition (‰) in species of Phylum Rhodophyta collected along Gulf of California coastlines.

Species (n composite samples)	δ^{13}C±SD (Min to Max, ‰)
Gracilaria sp. (18)	-15.5±2.4 (-21.8 to -12.2)
Gracilaria sp.2 (3)	-14.4±3.7 (-18.7 to -12.3)
G. crispata (7)	-15.1±3.0 (-19.1 to -10.1)
G. pacifica (6)	-16.5±1.6 (-18.6 to -13.6)
G. spinigera (3)	-14.9±3.8 (-17.7 to -12.2)
G. subsecundata (8)	-15.9±2.8 (-20.3 to -12.8)
G. tepocensis (3)	-15.1±1.9 (-17.0 to -13.2)
G. textorii (4)	-16.2±2.6 (-18.1 to -14.3)
G. turgida (5)	-15.3±3.6 (-20.7 to -12.0
G. vermiculophylla (16)	-15.9±3.8 (-23.4 to -8.8)
Hypnea sp. (14)	-14.9±2.6 (-20.9 to -11.4)
H. johnstonii (5)	-11.2±3.5 (-13.8 to -6.5)
H. pannosa (5)	-11.8±3.3 (-15.0 to -6.4)
H. spinella (6)	-16.4±1.8 (-19.2 to -14.9)
H. valentiae (6)	-15.2±2.3 (-19.2 to -12.7)
Laurencia sp. (8)	-12.9±1.2 (-14.7 to -10.5)
L. pacifica (8)	-14.9±2.2 (-19.0 to -12.7)
L. papillosa (3)	-15.7±0.3 (-15.9 to -15.6)
Spyrida sp. (5)	-17.1±1.12 (-19.1 to -16.1)
S. filamentosa (14)	-15.9±3.8 (-26.2 to -11.5)

Table 4. Summary of the estimated regression coefficients for each simple linear regression analyses and on the constant of fitted regression models. Estimated regression coefficients includes degrees of freedom for the error (DFE), root-mean-square error (RMSE), coefficients of determination (R^2) and the adjusted R^2 statistics, Mallow's Cp criterion (Cp), Akaike Information Criterion (AIC), Bayesian Information Criterion (BIC) minimum, F Ratio test, and p-value for the test (Prob > F). Models information includes value of the constant a ($\delta^{13}C$, ‰), standard error (SE), t ratio and Prob > |t| (values * are significant).

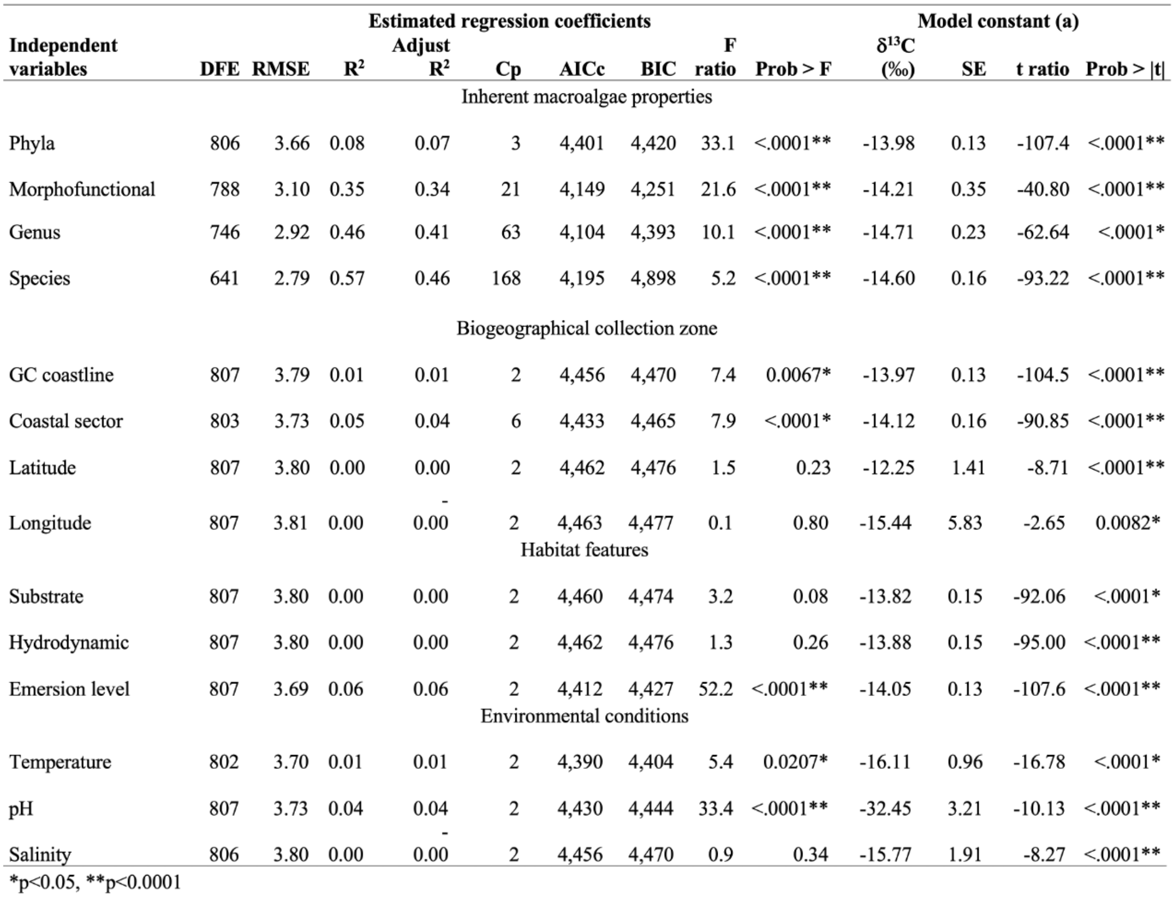

	Estimated regression coefficients									Model constant (a)			
Independent variables	**DFE**	**RMSE**	**R^2**	**Adjust R^2**	**Cp**	**AICc**	**BIC**	**F ratio**	**Prob > F**	**$\delta^{13}C$ (‰)**	**SE**	**t ratio**	**Prob > |t|**
Inherent macroalgae properties													
Phyla	806	3.66	0.08	0.07	3	4,401	4,420	33.1	<.0001**	-13.98	0.13	-107.4	<.0001**
Morphofunctional	788	3.10	0.35	0.34	21	4,149	4,251	21.6	<.0001**	-14.21	0.35	-40.80	<.0001**
Genus	746	2.92	0.46	0.41	63	4,104	4,393	10.1	<.0001**	-14.71	0.23	-62.64	<.0001*
Species	641	2.79	0.57	0.46	168	4,195	4,898	5.2	<.0001**	-14.60	0.16	-93.22	<.0001**
Biogeographical collection zone													
GC coastline	807	3.79	0.01	0.01	2	4,456	4,470	7.4	0.0067*	-13.97	0.13	-104.5	<.0001**
Coastal sector	803	3.73	0.05	0.04	6	4,433	4,465	7.9	<.0001*	-14.12	0.16	-90.85	<.0001**
Latitude	807	3.80	0.00	0.00	2	4,462	4,476	1.5	0.23	-12.25	1.41	-8.71	<.0001**
Longitude	807	3.81	0.00	-0.00	2	4,463	4,477	0.1	0.80	-15.44	5.83	-2.65	0.0082*
Habitat features													
Substrate	807	3.80	0.00	0.00	2	4,460	4,474	3.2	0.08	-13.82	0.15	-92.06	<.0001*
Hydrodynamic	807	3.80	0.00	0.00	2	4,462	4,476	1.3	0.26	-13.88	0.15	-95.00	<.0001**
Emersion level	807	3.69	0.06	0.06	2	4,412	4,427	52.2	<.0001**	-14.05	0.13	-107.6	<.0001**
Environmental conditions													
Temperature	802	3.70	0.01	0.01	2	4,390	4,404	5.4	0.0207*	-16.11	0.96	-16.78	<.0001*
pH	807	3.73	0.04	0.04	2	4,430	4,444	33.4	<.0001**	-32.45	3.21	-10.13	<.0001**
Salinity	806	3.80	0.00	-0.00	2	4,456	4,470	0.9	0.34	-15.77	1.91	-8.27	<.0001**

*p<0.05, **p<0.0001

Table 5. Summary of the estimated regression coefficients for each multivariate linear regression analyses and on their constant of fitted regression models performed in individuals binned by genus. Estimated regression coefficients include degrees of freedom for the error (DFE), root-mean-square error (RMSE), coefficients of determination (R^2) and the adjusted R^2 statistics, Mallow's Cp criterion (Cp), Akaike Information Criterion (AIC), Bayesian Information Criterion (BIC) minimum, F Ratio test, and p-value for the test (Prob > F). Model information includes value of the constant a ($\delta^{13}C$, ‰), standard error (SE), t ratio and Prob > $\lvert t \rvert$ (values * are significant).

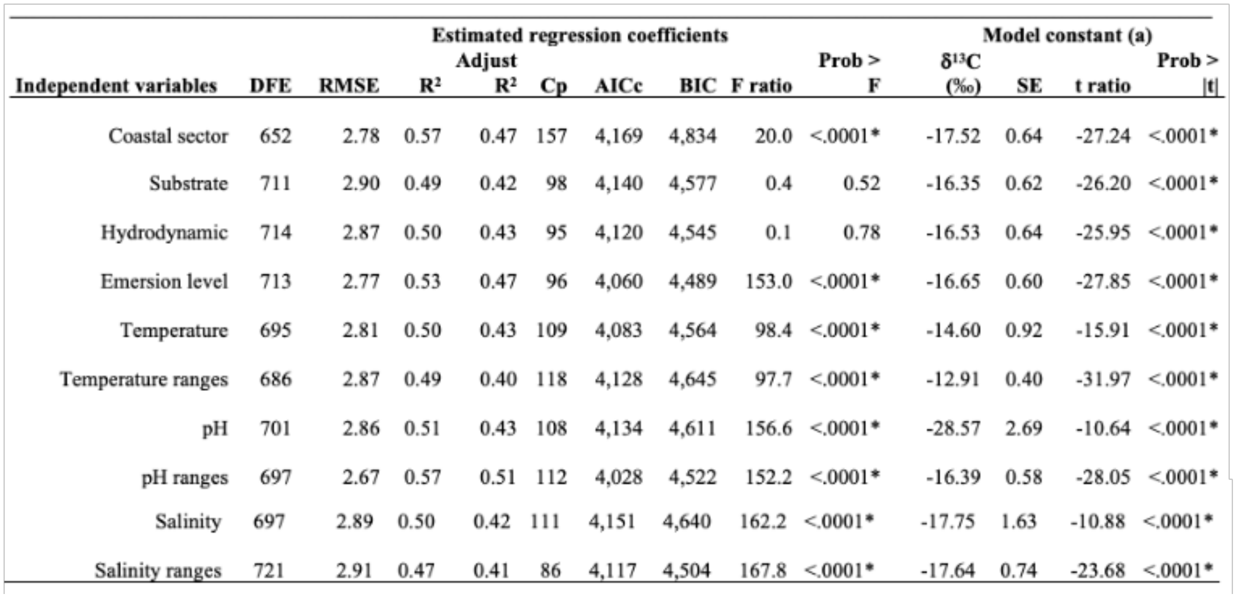

	Estimated regression coefficients									Model constant (a)			
Independent variables	**DFE**	**RMSE**	**R^2**	**Adjust R^2**	**Cp**	**AICc**	**BIC**	**F ratio**	**Prob > F**	**$\delta^{13}C$ (‰)**	**SE**	**t ratio**	**Prob > $\lvert t \rvert$**
Coastal sector	652	2.78	0.57	0.47	157	4,169	4,834	20.0	<.0001*	-17.52	0.64	-27.24	<.0001*
Substrate	711	2.90	0.49	0.42	98	4,140	4,577	0.4	0.52	-16.35	0.62	-26.20	<.0001*
Hydrodynamic	714	2.87	0.50	0.43	95	4,120	4,545	0.1	0.78	-16.53	0.64	-25.95	<.0001*
Emersion level	713	2.77	0.53	0.47	96	4,060	4,489	153.0	<.0001*	-16.65	0.60	-27.85	<.0001*
Temperature	695	2.81	0.50	0.43	109	4,083	4,564	98.4	<.0001*	-14.60	0.92	-15.91	<.0001*
Temperature ranges	686	2.87	0.49	0.40	118	4,128	4,645	97.7	<.0001*	-12.91	0.40	-31.97	<.0001*
pH	701	2.86	0.51	0.43	108	4,134	4,611	156.6	<.0001*	-28.57	2.69	-10.64	<.0001*
pH ranges	697	2.67	0.57	0.51	112	4,028	4,522	152.2	<.0001*	-16.39	0.58	-28.05	<.0001*
Salinity	697	2.89	0.50	0.42	111	4,151	4,640	162.2	<.0001*	-17.75	1.63	-10.88	<.0001*
Salinity ranges	721	2.91	0.47	0.41	86	4,117	4,504	167.8	<.0001*	-17.64	0.74	-23.68	<.0001*

Table 6. Summary of the estimated regression coefficients for each multivariate linear regression analyses and on their constant of fitted regression models performed in individuals binned by coastline sector and genus. Estimated regression coefficients include degrees of freedom for the error (DFE), root-mean-square error (RMSE), coefficients of determination (R^2) and the adjusted R^2 statistics, Mallow's Cp criterion (Cp), Akaike Information Criterion (AIC), Bayesian Information Criterion (BIC) minimum, F Ratio test, and p-value for the test (Prob > F). Model information includes value of the constant a ($\delta^{13}C$, ‰), standard error (SE), t ratio and Prob > |t| (values * are significant).

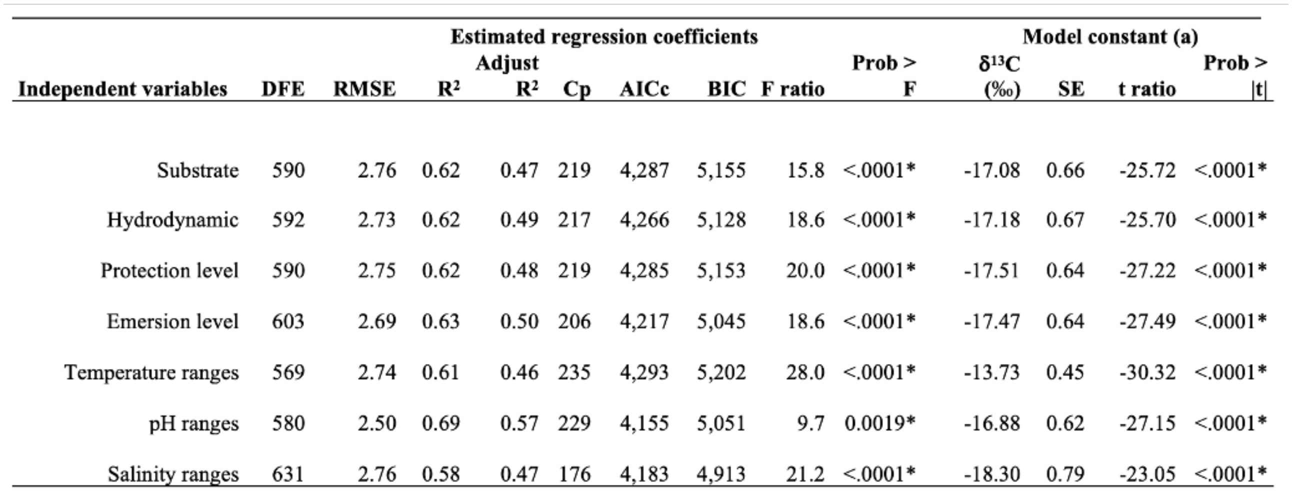

	Estimated regression coefficients									Model constant (a)			
Independent variables	**DFE**	**RMSE**	**R^2**	**Adjust R^2**	**Cp**	**AICc**	**BIC**	**F ratio**	**Prob > F**	**$\delta^{13}C$ (‰)**	**SE**	**t ratio**	**Prob > |t|**
Substrate	590	2.76	0.62	0.47	219	4,287	5,155	15.8	<.0001*	-17.08	0.66	-25.72	<.0001*
Hydrodynamic	592	2.73	0.62	0.49	217	4,266	5,128	18.6	<.0001*	-17.18	0.67	-25.70	<.0001*
Protection level	590	2.75	0.62	0.48	219	4,285	5,153	20.0	<.0001*	-17.51	0.64	-27.22	<.0001*
Emersion level	603	2.69	0.63	0.50	206	4,217	5,045	18.6	<.0001*	-17.47	0.64	-27.49	<.0001*
Temperature ranges	569	2.74	0.61	0.46	235	4,293	5,202	28.0	<.0001*	-13.73	0.45	-30.32	<.0001*
pH ranges	580	2.50	0.69	0.57	229	4,155	5,051	9.7	0.0019*	-16.88	0.62	-27.15	<.0001*
Salinity ranges	631	2.76	0.58	0.47	176	4,183	4,913	21.2	<.0001*	-18.30	0.79	-23.05	<.0001*

Table 7. Summary of the estimated regression coefficients for each multivariate linear regression analyses and on their constant of fitted regression models performed in individuals binned in coastline sector, habitats features, environmental conditions, and Physiological performed separately by morpho-functional groups and genus. Estimated regression coefficients include degrees of freedom for the error (DFE), root-mean-square error (RMSE), coefficients of determination (R^2) and the adjusted R^2 statistics, Mallow's Cp criterion (Cp), Akaike Information Criterion (AIC), Bayesian Information Criterion (BIC) minimum, F Ratio test, and p-value for the test (Prob > F). Model information includes value of the constant a ($\delta^{13}C$, ‰), standard error (SE), t ratio and Prob > |t| (values * are significant).

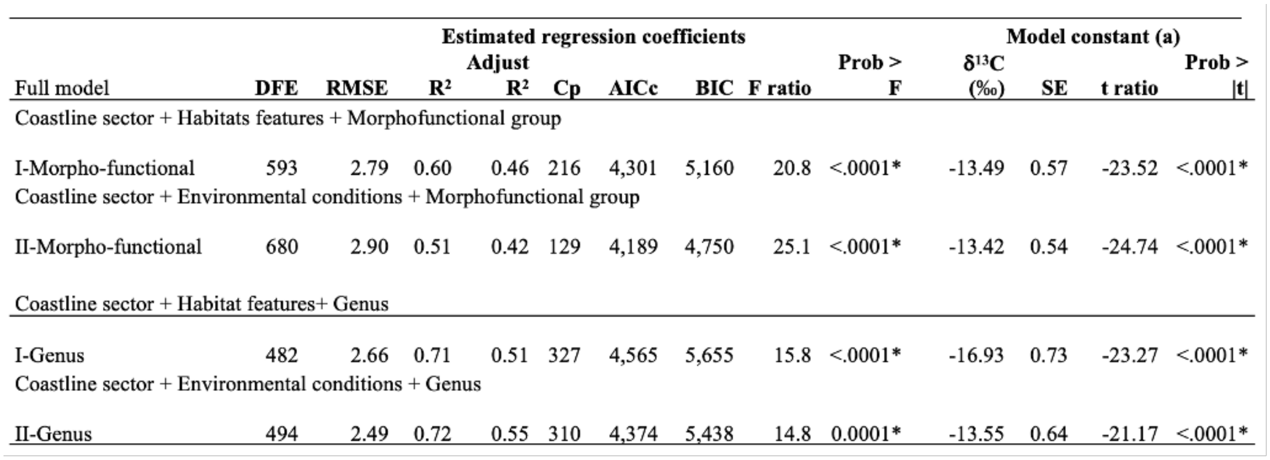

	Estimated regression coefficients									Model constant (a)			
Full model	DFE	RMSE	R^2	Adjust R^2	Cp	AICc	BIC	F ratio	Prob > F	$\delta^{13}C$ (‰)	SE	t ratio	Prob > |t|
Coastline sector + Habitats features + Morphofunctional group													
I-Morpho-functional	593	2.79	0.60	0.46	216	4,301	5,160	20.8	<.0001*	-13.49	0.57	-23.52	<.0001*
Coastline sector + Environmental conditions + Morphofunctional group													
II-Morpho-functional	680	2.90	0.51	0.42	129	4,189	4,750	25.1	<.0001*	-13.42	0.54	-24.74	<.0001*
Coastline sector + Habitat features+ Genus													
I-Genus	482	2.66	0.71	0.51	327	4,565	5,655	15.8	<.0001*	-16.93	0.73	-23.27	<.0001*
Coastline sector + Environmental conditions + Genus													
II-Genus	494	2.49	0.72	0.55	310	4,374	5,438	14.8	0.0001*	-13.55	0.64	-21.17	<.0001*

Table 8. Constant of fitted regression model explaining the $\delta^{13}C$ variability by morpho-functional groups. Model information includes value of the constant a ($\delta^{13}C$, ‰), standard error (SE), t ratio and Prob > |t|. Only morpho-functional groups with significant effects are enlisted.

Term	Estimated	SE	Razón t	Prob > |t|
Model constant	-14.2	0.4	-40.80	<.0001**
R-Smaller-sized articulated corallines	4.5	1.7	2.58	0.0100*
O-Compressed with branched or divided thallus	1.2	0.5	2.66	0.0079*
C-Erect thallus	1.8	0.6	2.84	0.0046*
R-Larger-sized articulated corallines	6.3	0.8	7.95	<.0001*
O-Hollow with spherical or subspherical shape	5.0	0.5	10.51	<.0001*
R-Blade-like with one of few layers of cells	-5.9	3.0	-1.98	0.0476*
C-Tubular	-1.6	0.5	-3.26	0.0012**
R-Filamentous uni&pluriseriate with erect thallus	-2.2	0.6	-3.92	<.0001*
R-Flattened macrophytes with cortication	-8.9	1.3	-7.10	<.0001*

*p<0.05, **p<0.0001

Table 9. Constant of fitted regression model explaining the $\delta^{13}C$ variability by genus. Model information includes value of the constant a ($\delta^{13}C$, ‰), standard error (SE), t ratio and Prob > |t|. Only genus with significant effects are enlisted.

Term	Estimated	SE	Razón t	Prob > |t|
Model constant	-14.7	0.2	-62.64	<.0001**
Corallina	6.4	2.9	2.22	0.0269*
Tacanoosca	3.5	1.3	2.71	0.0070*
Jania	5.0	1.7	2.97	0.0031*
Struveopsis	4.1	1.3	3.15	0.0017*
Codium	2.3	0.6	4.08	<.0001**
Padina	2.2	0.5	4.8	<.0001**
Hydroclathrus	7.3	1.1	6.59	<.0001**
Amphiroa	6.8	0.8	9.05	<.0001**
Colpomenia	5.4	0.4	14.02	<.0001*
Spyridia	-1.5	0.7	-2.10	0.0361*
Gracilaria	-0.9	0.4	-2.18	0.0294*
Polysiphonia	-3.7	0.8	-4.82	<.0001**
Schizymenia	-19.1	2.1	-9.33	<.0001**

*p<0.05, **p<0.001

Table 10. Constant of fitted regression model explaining the $\delta^{13}C$ variability by species. Model information includes value of the constant a ($\delta^{13}C$, ‰), standard error (SE), t ratio and Prob > |t|. Only genus with significant effects are enlisted.

Term	$\delta^{13}C$, ‰ estimated	SE	Razón t	Prob > |t|
Model constant	-14.6	0.2	-93.22	<.0001**
Hypnea pannosa	2.8	1.3	2.24	0.0256*
Colpomenia ramosa	3.2	1.4	2.27	0.0237*
Corallina vancouverensis	6.3	2.8	2.27	0.0238*
Caulerpa peltata	3.9	1.6	2.4	0.0165*
Codium sp.	3.0	1.3	2.4	0.0167*
Amphiroa misakiensis	7.1	2.8	2.55	0.0110*
Jania sp.	5.0	2.0	2.56	0.0106*
Codium brandegeei	2.8	1.1	2.63	0.0088**
Hypnea johnstonii	3.4	1.3	2.74	0.0063**
Tacanoosca uncinata	3.4	1.3	2.74	0.0062**
Struveopsis sp.	4.0	1.4	2.86	0.0044**
Padina durvillei	1.4	0.5	2.87	0.0043**
Amphiroa sp.*3*	8.2	2.8	2.95	0.0033**
Codium simulans	3.2	0.9	3.41	0.0007**
Amphiroa sp.2	6.6	1.6	4.1	<.0001**
Colpomenia sinuosa	4.4	1.1	4.17	<.0001**

Colpomenia sp.	3.6	0.9	4.27	<.0001**
Padina sp.	3.5	0.7	4.77	<.0001**
Hydroclathrus clathratus	7.2	1.1	6.82	<.0001**
Amphiroa sp.	8.1	0.9	8.67	<.0001**
Colpomenia tuberculata	5.9	0.4	15.45	<.0001**
Spyrida sp.	-2.5	1.3	-1.97	0.0496*
Pyropia thuretii	-5.5	2.8	-1.98	0.0480*
Ulva acanthophora	-1.2	0.6	-2.06	0.0399*
Grateloupia filicina	-2.4	1.1	-2.08	0.0382*
Rhodymenia sp.	-4.1	2.0	-2.08	0.0380*
Ulva compressa	-3.2	1.4	-2.33	0.0203*
Rhizoclonium riparium	-5.1	1.6	-3.15	0.0017**
Polysiphonia sp.	-4.8	1.4	-3.44	0.0006**
Halymenia actinophysa	-9.9	2.8	-3.57	0.0004**
Cladophora microcladioides	-7.2	2.0	-3.64	0.0003**
Polysiphonia mollis	-5.2	1.1	-4.93	<.0001**
Schizymenia pacifica	-19.2	2.0	-9.76	<.0001**

*p<0.05, **p<0.001

SUPLEMENTARY INFORMATION

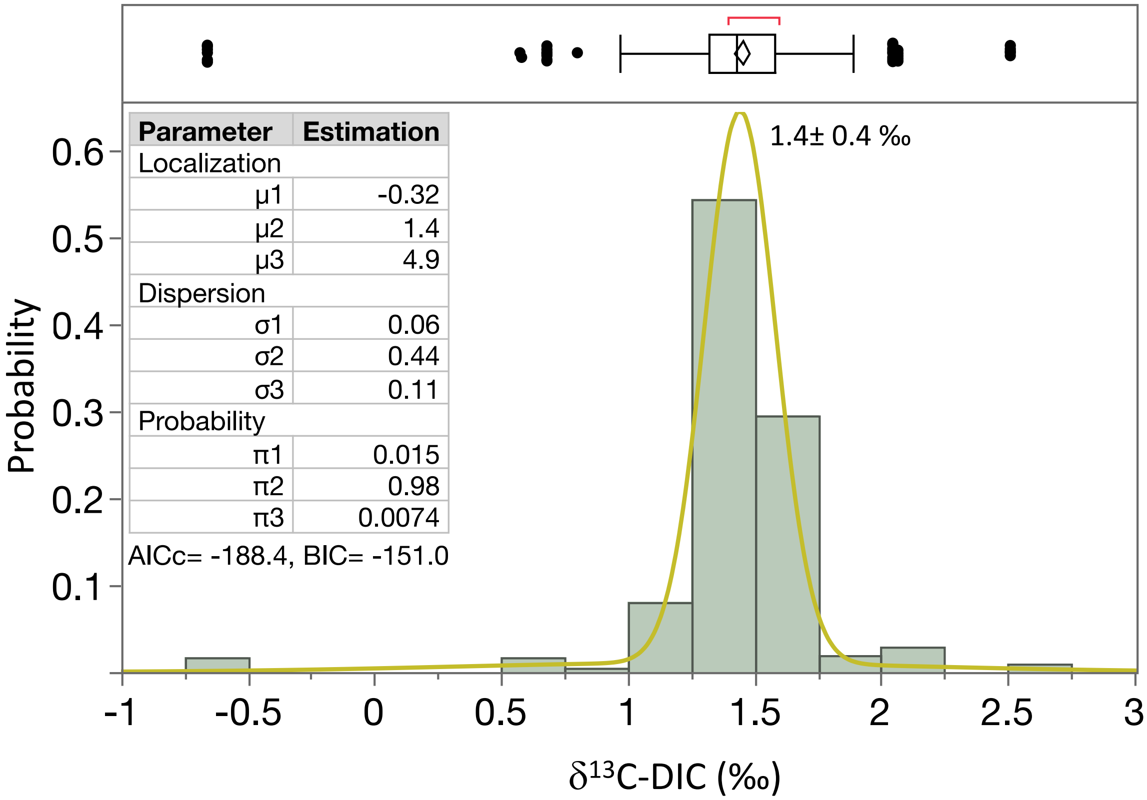

Parameter	Estimation
Localization	
μ1	-0.32
μ2	1.4
μ3	4.9
Dispersion	
σ1	0.06
σ2	0.44
σ3	0.11
Probability	
π1	0.015
π2	0.98
π3	0.0074

AICc= -188.4, BIC= -151.0

Fig. S1. Histogram representing the distribution of δ^{13}C-DIC values in surface seawater in the Gulf of California.

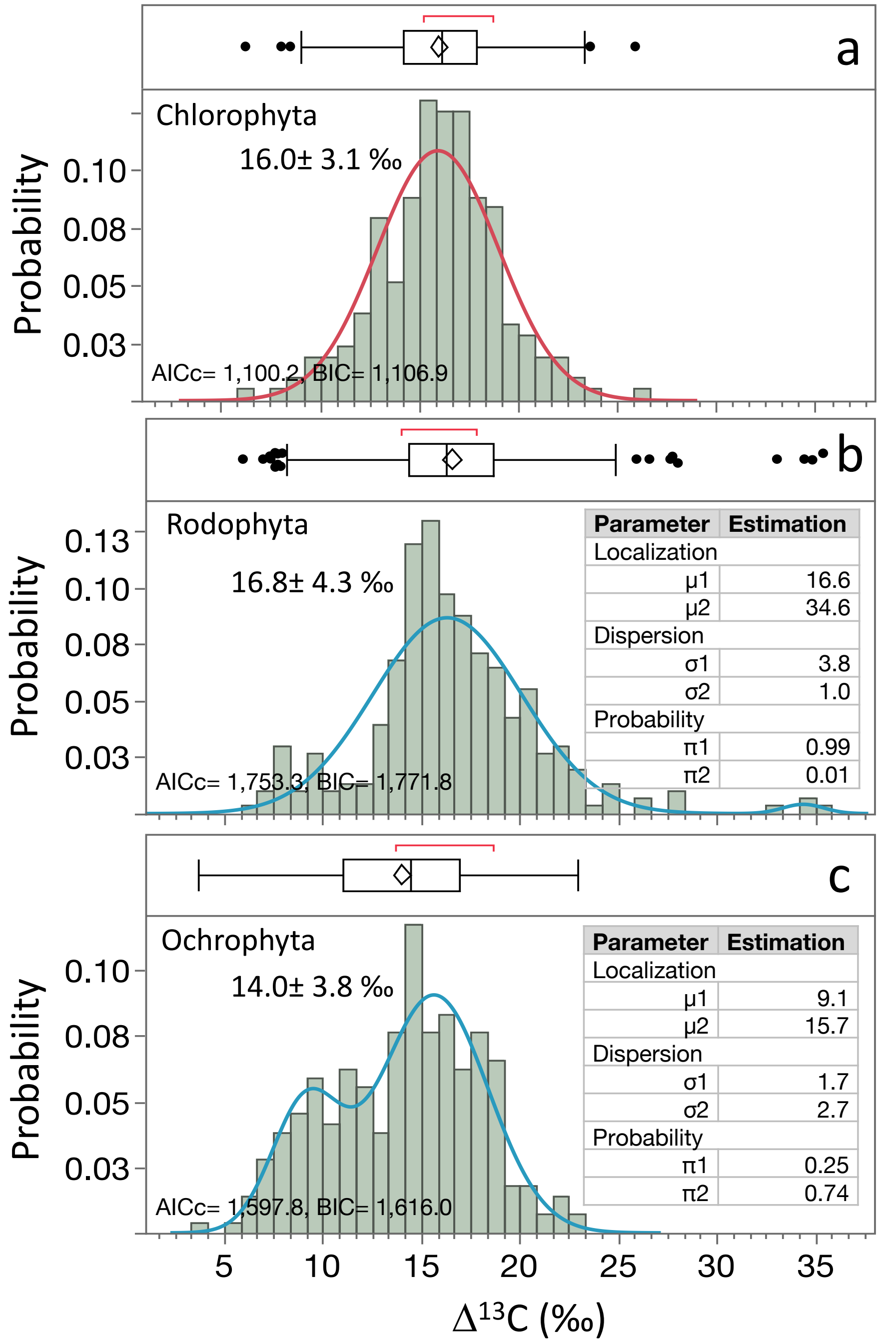

Parameter	Estimation
Localization	
μ1	16.6
μ2	34.6
Dispersion	
σ1	3.8
σ2	1.0
Probability	
π1	0.99
π2	0.01

Parameter	Estimation
Localization	
μ1	9.1
μ2	15.7
Dispersion	
σ1	1.7
σ2	2.7
Probability	
π1	0.25
π2	0.74

Fig. S2. Histograms representing the distribution of Δ^{13}C-macroalgal in macroalgae collected in the Gulf of California for Phyla a) Chlorophyta, b) Rhodophyta, and c) Ochrophyta.